# Eruptive YSOs in Cygnus-X: a mid-infrared variability study with NEOWISE and SPICY

C. Morris[1]⋆ Z. Guo[2,3,1], P. W. Lucas[1], N. Miller[1,4], C. Contreras-Peña[5,6] and M. A. Kuhn[1]

[1]*Centre for Astrophysics Research, University of Hertfordshire, College Lane, Hatfield, Hertfordshire, AL10 9AB, UK*

[2]*Instituto de Física y Astronomía, Universidad de Valparaíso, ave. Gran Bretaña, 1111, Casilla 5030, Valparaíso, Chile*

[3]*Millennium Institute of Astrophysics, Nuncio Monseñor Sotero Sanz 100, Of. 104, Providencia, Santiago, Chile*

[4]*Department of Physics & Astronomy, University of Wyoming, 1000 E. University, Laramie, WY 82070, USA*

[5]*Department of Physics and Astronomy, Seoul National University, 1 Gwanak-ro, Gwanak-gu, Seoul 08826, Republic of Korea*

[6]*Research Institute of Basic Sciences, Seoul National University, Seoul 08826, Republic of Korea*

## ABSTRACT

The mass accretion process controls the pre-main-sequence evolution, although its unstable characteristic has yet to be fully understood, especially towards the young protostellar stage. In this work, we have undertaken a thorough examination of the mid-infrared variability of Spitzer-selected YSOs in the Cygnus-X star-forming region over the last decade, using the *NEOWISE* time series. This work compares two groups of young stars: embedded Class I objects, and the more evolved flat-spectrum/Class II sources. We report on 68 candidate eruptive variables within these groups, including 17 with characteristics that resemble the photometric behaviour of FUors. We find the candidate FUors to be an order of magnitude more common among the younger Class I systems than more evolved objects. A large number of the identified short-duration eruptive YSOs display mid-infrared colour behaviour that is redder-when-brighter, which contrasts with optically bright outbursts seen in YSOs. Finally, we note the unusual long-term rising behaviours of four Class I YSOs, with rising timescales longer than five years, which is far slower than ~6-12 month timescale for the majority of optically discovered FUors.

**Key words:** stars: pre-main sequence – stars: protostar – stars: variables: T Tauri – infrared: stars

## 1 INTRODUCTION

The pre-main-sequence evolution of low-mass stars consists of four stages (from Class 0 to III), defined by the relative brightness of the stellar photosphere and the circumstellar disc or envelope (Greene & Lada 1996). Class 0 and Class I sources are the earliest evolutionary stages, so-called protostars, during which the young star is embedded in its envelope and optically invisible. During the more evolved Class II stage, the young stellar object (YSO) is directly observable at optical wavelengths, accompanied by active accretion funnel flows linking the circumstellar disc and the stellar surface (Bouvier et al. 2007). Additionally, the "flat-spectrum" stage (FS) is defined as the transitional stage between Class I and II, where the stellar photosphere and accretion disk share similar luminosity, namely a flat spectral energy distribution (SED). Quantitatively, these pre-main-sequence evolutionary stages were classified by the near to mid-infrared spectral index $\alpha$, as Class I ($\alpha > 0.3$), FS ($-0.3 < \alpha < 0.3$), and Class II ($\alpha < -0.3$). Previous photometric surveys have revealed that the mass accretion process on YSOs has an unstable characteristic (e.g. Stauffer et al. 2014; Venuti et al. 2019; Contreras Peña et al. 2020). However, most past works focused on the optical to near-infrared variability of Class II YSOs. Systematic monitoring of the accretion variability of protostellar cluster members will shed light on the

accretion variability towards earlier evolutionary stages, where the average accretion rate is higher than in the FS and Class II stages.

The long duration time coverage of mid-infrared (MIR) surveys, by Spitzer, WISE and the current NEOWISE (Hora et al. 2007; Wright et al. 2010; Mainzer et al. 2014), provides the ability to find variable events on multi-year timescales. The nearby massive star-forming complex of Cygnus-X (at roughly 1.4 kpc, Rygl et al. (2012)) makes an excellent test site for studying the long-term behaviour of YSOs, because of the wide range of surveys it is included within. These surveys cover multiple wavelengths with a long time baseline, providing a high completeness of YSO candidates in the region. The large sample of Kryukova et al. (2014b), which identifies over 2000 candidate YSOs, utilised the full MIR coverage provided by *Spitzer* to isolate YSO candidates on the basis of MIR colour; these sources are exclusively Class I YSOs with a *[24]* detection. The same sky region is also covered by NEOWISE, The UKIRT Galactic Plane Survey (UGPS) (Lucas et al. 2008), the Two Micron All-Sky Survey (2MASS) (Skrutskie et al. 2006), *Gaia* (Gaia Collaboration et al. 2023), and the INT Photometric Hα Survey (IPHAS) (Barentsen et al. 2014; Drew et al. 2005).

In addition, there is a large list of YSO candidates available in the Cygnus-X region, from the *Spitzer*-based SPICY (Kuhn et al. 2021) catalogue of YSOs. SPICY uses a mixture of traditional infrared colour cuts and random forest classifiers to produce a comprehensive list of Class II and flat-spectrum YSOs in the 613 deg$^2$ covered by

⋆ E-mail: c. morris6@herts.ac.uk

the existing cryogenic-era Glimpse surveys (Benjamin et al. 2003; Whitney et al. 2011). It contains a large number of Class I YSOs and a reduced number of Class III sources owing to the much lower IR excess of those stars. In this instance, there are 7281 additional YSOs, to those found in the aforementioned sample from the Cygnus-X Legacy Survey (Beerer et al. 2010; Kryukova et al. 2014b)[1]. Given the broad wavelength coverage of the region, there lies an opportunity to investigate the range and frequency of both high amplitude variability generally and eruptive variability specifically, for YSOs at different evolutionary stages.

The post-reactivation NEOWISE survey provides an opportunity to study the long-term time-domain behaviour of YSOs. The NEO-WISE survey covers the whole sky in both the 3.4 $\mu$m $W1$ and 4.6 $\mu$m $W2$ bands. At present, there have been over 10 years of continuous monitoring, at ~6 month intervals, comprised of many single scans. Considering the higher brightness at 24 $\mu$m of the Class I protostars, our sample of Class I YSOs will preferentially target the younger objects. Such a search for eruptive variables (EVs) at the protostellar stage has not been previously carried out within Cygnus-X.

Variability is a common characteristic among YSOs. This is often of a low amplitude nature (<1 mag in optical), driven by small changes in extinction along line-of-sight, accretion rate, or by stellar rotation. Alternatively, unpredicted high-amplitude accretion events are observed on young stars, during which YSOs accrete a significant portion of their final mass (see Hartmann & Kenyon 1996). These bursts have a myriad of different triggering mechanisms, with theoretical studies able to reproduce outbursts via: Gravitational Instability (GI) and Magneto-Rotational Instability (MRI) in the inner disk (Kratter & Lodato 2016; Bourdarot et al. 2023), thermal instabilities (Bell & Lin 1994; Nayakshin & Elbakyan 2024), disk fragmentation, either due to GI (Vorobyov & Basu 2010), or young massive planets (Clarke et al. 2005), stellar flybys (Cuello et al. 2019; Borchert et al. 2022b) and evaporating young hot Jupiter (Nayakshin et al. 2024). This wide range also ensures that there is no universal model for an episodic accretion event, and thus large observationally confirmed samples of these events will be required to understand them further.

Observationally, the young accretion bursts are traditionally characterised into two distinct groups, based on their duration and amplitude. The FUor-type, named after FU Ori, are long-lasting (order of decades or centuries) outbursts of high amplitude and a comparatively short brightening time scale, on the order of ~1000 days (Hartmann & Kenyon 1996). These outbursts are considered rare, with only a few dozen confirmed by both spectroscopy and photometry (Connelley & Reipurth 2018), including those recently identified by VVV and Gaia time series photometry (such as Contreras Peña et al. 2017a; Lucas et al. 2024; Guo et al. 2024a,b; Hillenbrand et al. 2018). The recurrence timescales of FUors are on the order of $10^5$ years (Scholz et al. 2013). These outbursts are driven by massively enhanced accretion, which will then cause the inner accretion disk to become self-luminous via viscous heating, and outshine the young star's photosphere, hence the distinctive spectrum of these objects (Zhu et al. 2009; Hartmann et al. 2011; Liu et al. 2022). Unlike FUors, another type of young outburst is called EXors, which has a much shorter outburst duration between months and a few years and a symmetric rising/cooling light curve morphology (Lorenzetti et al. 2012). Some EXors have repeated outbursting behaviour on a time scale of decade (Kuhn et al. 2023) and some others may be periodic (Guo et al. 2022). Uniform amongst EXors is that the

YSOs maintain magnetospheric accretion, with spectra frequently containing Hı emission lines. Recently, a much wider array of outbursting behaviours has been noted among eruptive YSOs (reviewed by Fischer et al. 2022), consisting of YSOs with photometric features similar to FUors, but with spectroscopic traits more comparable to EXors (see Briceño et al. 2004; Acosta-Pulido et al. 2007). The range of behaviours is further challenged by the near-infrared VVV survey (Minniti et al. 2010; Guo et al. 2021), where the majority of long-duration outbursts (>10 years) were displaying EXor-like magnetospheric accretion signatures in their spectra.

The incidence rate of eruptive variability in YSOs is a subject of importance when considering the 'protostellar luminosity spread problem', but the variance in amplitude (with respect to the photometric bandpasses being used for observations) has not been probed in detail previously. Statistical studies using large-scale photometric surveys revealed that accretion outbursts are more common at younger stages, with a lower occurrence rate towards more evolved systems (see Contreras Peña et al. 2024). However, driven by the larger amplitudes observed in the optical and near-IR (as compared to those found in the MIR), YSOs with a less massive envelope are easier to detect during the outburst, leading to a bias on the estimated number density. A sample of nearby YSOs, selected from the MIR NEOWISE photometry, is desired to examine the range of eruptive behaviours towards the younger evolutionary stage. We have performed a detailed survey to monitor the long-term time-domain behaviour of these young systems, providing insight into how common the traditional FUor and EXor variables might be among a MIR-selected population, or if other eruptive events will dominate.

In this work, we will present two selections of YSOs within the region of Cygnus-X: one of embedded objects with a 24 $\mu$m detection, mostly Class I YSOs with a small number of FS stars. The other is comprised of non-embedded flat-spectrum and Class II/III sources (likely without envelopes). The details of our sample selection methods and data processing procedures are presented in §2. In §3 we will discuss individual eruptive variables of interest within each selection. Then in §4 we will compare the incidence of eruptive variability (and of the FUor phenomenon in particular) between both populations and of similar sources from the literature.

## 2 SAMPLE SELECTION AND DATA PROCESSING

In this section, we will present the data products applied in this work, including archived data products from the WISE satellite and PI observations for highlighted sources. We will also introduce our selection methods to identify eruptive YSOs among the members of the Cygnus-X star-forming region.

### 2.1 Archived WISE data

We obtained NEOWISE light curves from the NASA/IPAC InfraRed Science Archive for the 2007 YSO candidates in Cygnus-X (Kryukova et al. 2014a), among which 1552 sources have valid detections in both $W1$ and $W2$. Of these 1552 sources, 1332 (these forming our first sample) have detections in at least 50% of the possible epochs of single scan data. Then, for each light curve, the NEOWISE single-scan data were combined with the earlier WISE measurements (ALLWISE, WISE 3-Band Cryo, and Post-Cryo, where available, acquired from the ALLWISE Multi-Epoch Photemetry Table). The photometry from the individual scans was then cleaned by removing detections with a high psf error. Additionally, those points with either *w1snr* or *w2snr* <5 were subject to cuts first used in Koenig &

---

Leisawitz (2014):

$$w1rchi2 < \frac{w1snr - 3}{7}, \qquad (1)$$

$$w2rchi2 < (0.1 \times w2snr) - 0.3. \qquad (2)$$

Data points that did not pass either criterion were not included in the per epoch median magnitudes. The error bars were taken as the standard deviation for the cleaned single-scan images at each epoch, rather than the stated photometric error in the catalogue. This change was motivated by the spread in fluxes at each epoch being larger than the stated errors, which may be indicative of an underlying underestimate of errors in the NEOWISE data. Additional data cleaning involved removing photometric measurements associated with quality control flags attributed to the frame itself ('qual_frame' ≠ 0) or those had measured fluxes as upper limits only.

To remove any bias associated with the selection of more heavily embedded YSOs (as well as investigating the distribution of EVs within this regime), a counterpart sample of sources was selected from the SPICY catalogue (Kuhn et al. 2021), featuring all candidate YSOs within the sky area used by Kryukova et al. (2014a), that did not feature in those authors' sample. This SPICY sample includes 7281 stars that were not recognised by Kryukova et al. (2014a), of which 5592 possess NEOWISE light curves, and 4935 have data of sufficient quality for analysis. We deem that a star must have data in at least 40% of epochs to reliably analyse in this regard.

Both the binned (the median of each scan within a single observation window) and unbinned light curves in the first sample (1332) were visually inspected to locate eruptive YSOs. Eruptions were considered for stars with amplitudes of over 1 magnitude (corresponding to ~2 mag in optical band-passes), and obvious brightening from a quiescent state. The list of targets for inspection was shortened to include only those targets with peak amplitudes of > 1 mag in either $W1$ or $W2$ bands (299). Some sample members were further examined via the inspection of their unTimely (Meisner et al. 2023) light curves, generated with the untimely catalogue tool (Kiwy 2022). The untimely catalogue is the time series of unWISE (Meisner et al. 2018), which stack the individual NEOWISE sky-passes to create deeper (~ 1.3 mag) per epoch images, using the crowdsource source detection and photometry software (Schlafly et al. 2018). The sources examined here were those with clearly variable light curves but with either high photometric error or a number of non-detections.

Candidate long-duration eruptive YSO outbursts were identified by fitting the light curves to a characteristic shape, defined by the rising slope, and a post-outburst linear decay. The two-component rising slope is defined in equations 3 & 4, as listed in Lucas et al. (2024):

$$m(t) = m_q - \frac{s}{1 + e^{-(t-t_0)/\tau}} \quad \text{where } t < t_0, \qquad (3)$$

$$m(t) = m_q - s(0.5 + 0.25(t-t_0)/\tau) \quad \text{where } t_0 \leq t \leq t_0 + 2\tau, \quad (4)$$

where m(t) is magnitude as a function of time ($t$), $m_q$ is the magnitude at quiescence, $t_0$ is the time at which the star is at half the peak amplitude ($s$), and $\tau$ is the e-folding timescale. The fitting combines the above slope with a linear decay that runs from $t_0 + 2\tau$ to the end of the time axis. The fit itself makes use of scipy's curvefit routine, using the above model, to fit the initial guesses for five free parameters ($\tau$, $t_0$, $m_q$, $s$ & the final magnitude), that are then fit by emcee over 10000 iterations (this code is now packaged as part of aptare[2]).

---

[2] Available at https://github.com/nialljmiller/Aptare

The sources with the lowest reduced mean squared error are then inspected to confirm as the FUor-type (examples are presented in Appendix A). This method does struggle to identify sources with bursts at the start of the NEOWISE monitoring window, as well as those that are currently rising (or very recently finished), such as Source 2003. It should be noted that all stars that were identified as EV candidates by visual inspection were still subject to analysis, and that this fitting method was trialed to locate YSOs resembling classical FUors.

We also utilised the two-epoch UGPS survey (Lucas et al. 2008) to identify YSOs with earlier outburst events (these being between 2011 and 2012) than would be seen between the epochs of the *Spitzer* Cygnus-X Legacy Survey and ALLWISE/NEOWISE surveys. We selected members of the Kryukova et al. (2014a) catalogue featuring a detection in 50% of UGPS images, then visually inspected the images to confirm genuine variability. This search identified 15 candidates, of which 11 were of sufficiently high amplitude (> 2 mag in $K$) to be considered eruptive. Of those 11, only two were not picked up by the NEOWISE search method (see §3).

### 2.2 Additional Data Products

We present three $K$-bandpass spectra of two candidate EVs identified via the large flux differences between two photometric epochs of the UKIDSS survey (Lucas et al. 2017). Two spectra were obtained by the Near-Infrared Integral Field Spectrometer (NIFS) mounted on the Gemini North telescope (McGregor et al. 2003), in June and December 2013. Another spectrum was observed in July 2017 with the Infrared Camera and Spectrograph (IRCS) installed at the Subaru telescope (Tokunaga et al. 1998; Kobayashi et al. 2000). The IRCS spectrum was reduced using the standard twodspec routines within iraf, and it has a resolution of 6.1 per pixel. The NIFS spectra were originally reduced and part of the published PhD thesis of Carlos Contreras-Peña (Contreras Peña 2015).

### 3 RESULTS

We present 68 candidate eruptive variables (EVs), across the groups with MIPS [24] detections and the SPICY selected stars without. They are to be split into three classifications based on their outburst timescales (which are predicted in instances where the latest event is ongoing). The three groups are: 'Long-Duration' of >10 years (LDE), 'Intermediate-Duration' of $2 \leq t \leq 10$ years (IDE), and 'Short-Duration' which are <2 years (SDE). Overall we identify 13 'Long-Duration' YSO outbursts, with 9 of 'Intermediate-Duration' and 41 'Short-Duration' events (these events were solely identified by eye). A final five of the YSOs with ongoing outbursts at the final epoch had not been active long enough to classify in this way, and are listed as 'ambiguous'.

### 3.1 Stars with MIPS [24] detection

There are 33 EVs that have MIPS [24] detection (which can be viewed in Table 2.2), and are have an ID derived from the Vizier row number for the Kryukova et al. (2014a) catalogue. Most of the stars are Class I YSOs (28) and a small number of FS sources (5). The FS sources in this sample require $[3.6] - [4.5] \geq 0$, as per Kryukova et al. (2014a). These sources were sorted into the three aforementioned categories based on the outburst timescale, as 11 long-duration, 8 intermediate-duration, and 11 short-duration outbursts. There are a final 3 stars that are of an ambiguous categorisation: sources 2003,

**Table 1.** List of outbursting Cygnus-X members from Kryukova et al. (2014a).

| Source Number | RA (deg) J2000 | Dec (deg) J2000 | $\Delta W1$ mag | $(W1-W2)_{min}$ mag | Spectral Index $\alpha$ | Timescale Class | Outburst Duration yr | Outburst Rise Time yr |
|---|---|---|---|---|---|---|---|---|
| 12* | 304.3677 | +41.9736 | 2.004 ± 0.019 | 1.01 | 1.03 | SDE | - | - |
| 121* | 305.5600 | +37.4743 | 1.848 ± 0.038 | 1.73 | 1.61 | SDE | - | - |
| 185 | 305.8536 | +37.5706 | 2.037 ± 0.07 | 3.05 | -0.08 | SDE | - | - |
| 232 | 306.0890 | +42.2683 | 1.692 ± 0.01 | 1.54 | 0.44 | SDE | - | - |
| 257† | 306.1356 | +37.8303 | 3.279 ± 0.013 | 1.65 | 1.23 | LDE | 24 | 2 |
| 294* | 306.2141 | +38.4203 | 2.524 ± 0.020 | 0.77 | 1.2 | LDE | >30 | 7 |
| 333 | 306.3550 | +39.3400 | 2.055 ± 0.011 | 1.33 | 0.4 | SDE | - | - |
| 352* | 306.4325 | +38.1869 | 1.795 ± 0.020 | 2.82 | 1.52 | SDE | - | - |
| 362** | 306.4640 | +39.3760 | 2.402 ± 0.023 | 1.86 | 0.58 | LDE | >10 | ? |
| 387* | 306.5333 | +41.6357 | 2.437 ± 0.097 | 1.97 | 0.27 | SDE | - | - |
| 397 | 306.5526 | +39.2783 | 2.262 ± 0.020 | 2.414 | 1.14 | IDE | 7-10 | > 3 |
| 441 | 306.6371 | +37.7786 | 1.674 ± 0.010 | 1.55 | 0.44 | SDE | - | - |
| 456 | 306.6672 | +40.0418 | 0.978 ± 0.016 | 0.7 | 0.16 | SDE | - | - |
| 591 | 306.9916 | +40.1975 | 2.354 ± 0.069 | 1.664 | 0.72 | LDE | >30 | 2 |
| 625 | 307.0390 | +40.1518 | 3.371 ± 0.031 | 1.32 | 0.2 | IDE | 4 | <1 |
| 658 | 307.1304 | +41.8473 | 1.749 ± 0.011 | 1.26 | 0.27 | IDE | 5 | ≈1 |
| 769 | 307.4425 | +39.2864 | 2.817 ± 0.050 | 1.95 | 0.66 | SDE | - | - |
| 812 | 307.5106 | +40.3149 | 3.571 ± 0.046 | 1.93 | 1.54 | IDE | 6 | <0.6 |
| 880 | 307.7106 | +41.2442 | 2.634 ± 0.030 | 1.27 | 0.22 | LDE | >10 | ? |
| 912 | 307.7863 | +40.0635 | 2.860 ± 0.036 | 2.732 | 0.88 | LDE | >30 | 5 |
| 1017 | 308.0107 | +40.3108 | 2.313 ± 0.165 | 2.39 | 1.14 | IDE | 6 | ≈1.5 |
| 1048 | 308.0877 | +41.1318 | 3.981 ± 0.511 | 1.733 | 1.7 | LDE | >30 | 7 |
| 1475 | 309.0957 | +39.6769 | 2.210 ± 0.053 | 2.81 | 1.19 | LDE | >30 | 1 |
| 1562 | 309.3483 | +42.2458 | 3.081 ± 0.062 | 2.49 | 1.01 | IDE | 3 | <1 |
| 1626 | 309.5138 | +42.5483 | 3.081 ± 0.008 | 1.16 | 0.09 | SDE | - | - |
| 1738 | 309.8197 | +42.2693 | 2.401 ± 0.027 | 2.49 | -0.05 | Amb | ? | ? |
| 1769* | 309.9753 | +42.0143 | 2.878 ± 0.008 | 2.27 | 1.15 | Amb | ? | ? |
| 1884 | 310.3783 | +41.9181 | 1.438 ± 0.01 | 0.569 | 1.77 | IDE | 5.5 | 3 |
| 1945 | 310.6990 | +42.7017 | 3.26 ± 0.041 | 1.961 | 0.77 | LDE | 10 | 3 |
| 1964** | 310.8678 | +42.8167 | 0.767 ± 0.007 | 1.517 | 0.82 | LDE | >10 | ? |
| 1991* | 310.9918 | +42.8032 | 3.035 ± 0.056 | 2.827 | 0.96 | LDE | 9? | 7 |
| 1999 | 311.0531 | +41.6165 | 4.606 ± 0.158 | 2.35 | 0.96 | IDE | 8 | 1.8 |
| 2003 | 311.0754 | +41.6140 | 5.089 ± 0.017 | 1.67 | 1.01 | Amb | ? | ? |

LDE: long-duration eruptive sources with fast-rising FUor-type morphology and/or with outburst duration > 10 yr.
IDE: intermediate-duration events with a duration between 2 - 10 yrs. SDE: short-duration events including stochastic and quasi-periodic eruptive sources.
Amb: ongoing outburst with ambitious duration. †: Source 257 is included in Contreras Peña et al. (2023).
*: the *Spitzer* detection is a blend between two detectable sources in UGPS. **: Sources previously found by the two-epoch UPGS photometry.

1738, & 1769. The former has an outstanding amplitude (> 5 mag in $W1$), but as per the latest NEOWISE release the outburst is still ongoing, and thus of an unknown type and duration. By contrast, Sources 1738 & 1769 have had multiple events observed in their light curves. For both systems one burst appears as a long/intermediate duration type (ongoing as of 2024), and the other was a short-duration burst. Two additional stars (Sources 362 and 1964) are included in this group which were detected as candidate eruptive stars via the two-epoch UGPS survey (Lucas et al. 2008). All eruptive targets can be found in Table 2.2.

### 3.1.1 Long-Duration Eruptive YSOs

Within the group of 11 eruptive variables with variability timescales greater than ten years, we note the presence of four stars with morphologies with similarities to those of classical FUors (Numbers: 257, 294, 591, & 1475, see Figures 1 & B1) i.e with a high amplitude outburst, that increases in brightness comparatively fast when compared to the following long duration decay. All display a high amplitude increase in luminosity over a 1 - 5 yr period, followed by a

plateauing that appears set to continue long into the future. Sources 257 and 294 show no signs of post-outburst fading, whereas source 1475 has an estimated fading timescale of ≈ 24 years assuming a linear decaying slope. Source 257 appears of a V1647 Ori-type on the strength that it has the characteristic emission spectrum in contrast to a FUor-type observed outburst. This source has been published in Contreras Peña et al. (2023), under the identifier SPICY 109331. This star makes an excellent test case for the other members of this group, with such features as a high-amplitude (3.28 mag) burst in $W1$, rising over a short time-frame of ∼ 2 years, and becoming steadily bluer in its MIR colour, which is also seen in both FUors and V1647 Ori objects.

In addition to the sources identified by their MIR eruptive behaviour, two further LDE candidates were identified on the basis of outbursts observed between the UKIDSS UGPS (Lucas et al. 2008) NIR images (sources 362 and 1964). Both were identified by searching for bursts of at least 2 mag, wherein one UGPS epoch had a non-detection and the other had a minimum brightness of 15 mag (2 mag above the lower limit of the survey). In each case, the lower limit for the non-detection was calculated for the relevant UGPS image, using the `ImageDepth` tool within the `Photutils` package
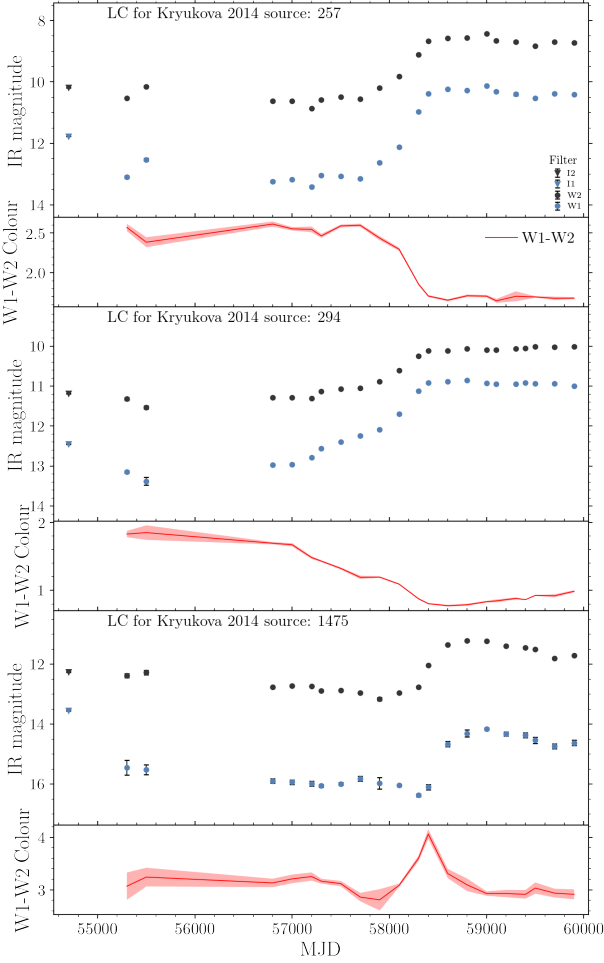
**Figure 1.** NEOWISE $W1$ & $W2$ light curves for three of the candidate eruptive variables with FUor type light curve morphologies. Each plot also contains a $W1 - W2$ colour indicator (red line), with the error included as the pink-shaded region.
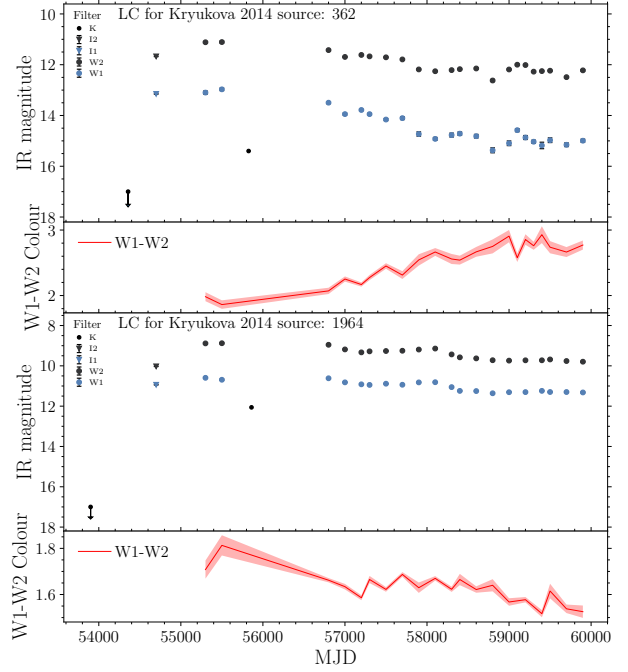


**Figure 2.** NEOWISE $W1$ & $W2$ light curves for the two LDE candidates identified with UGPS photometry. The arrows represent the upper limits of UGPS for each field.

### 3.1.2 Intermediate Duration Eruptive YSOs

We identify eight stars in this sample with outbursts that are within the 2 to 10 yr boundary we set for the 'Intermediate-Duration Eruptive' (IDE) group. Of these, three targets (Sources 812, 1884 and 1999) have morphologies that resemble a FUor-type event (see Figure 4), but are shorter than the >20-year timescales expected for FUors and are similar in morphology (if not amplitude) to VVV1636-4744 and L222_4 from Guo et al. (2024a). The two stars from Guo et al's sample have similar rise times (∼500 days) & NIR amplitudes of 4 mag and 6 mag respectively, but have differing spectral characteristics. L222_4 presents a typical red, absorption spectrum, typical of FUors, whereas VVV1636-4744 has an emission line dominated spectrum, more like EX Lup. Two further IDEs have completed outbursts (Sources 397 and 1017, Figure C1). The final three IDEs (Sources 625, 658 & 1562, in Figure C2) have a multi-peaked shape to their light curves that do not resemble those of FUors.

Of the stars that resemble shorter duration FUors, we found some key differences between each star. For example, Source 812 displays at least 5 yr of a gradual increase in luminosity, before a very short (<6 months) outburst. This behaviour is similar to FUors like Gaia17bpi (with the 2-stage initial outburst) as discussed earlier. Source 1999 has the second largest outburst in the sample but displays a much steeper decay slope than the three stars mentioned previously, indicative of a shorter outburst duration than most classical FUors, but longer than classical EXors (estimated at ≈8 years). Finally, Source 1884 has the second lowest amplitude of the stars in this group at 1.44 mag (with a gradient of ≈ 0.36 mag yr$^{-1}$), but this is combined with the bluest quiescent $W1 - W2$ colour (between 1.11 mag and 0.56 mag). Given the range in spectra seen in Guo et al. (2024a), acquiring NIR spectra for these three sources is essential in ascertaining the nature of the outbursts we have observed.
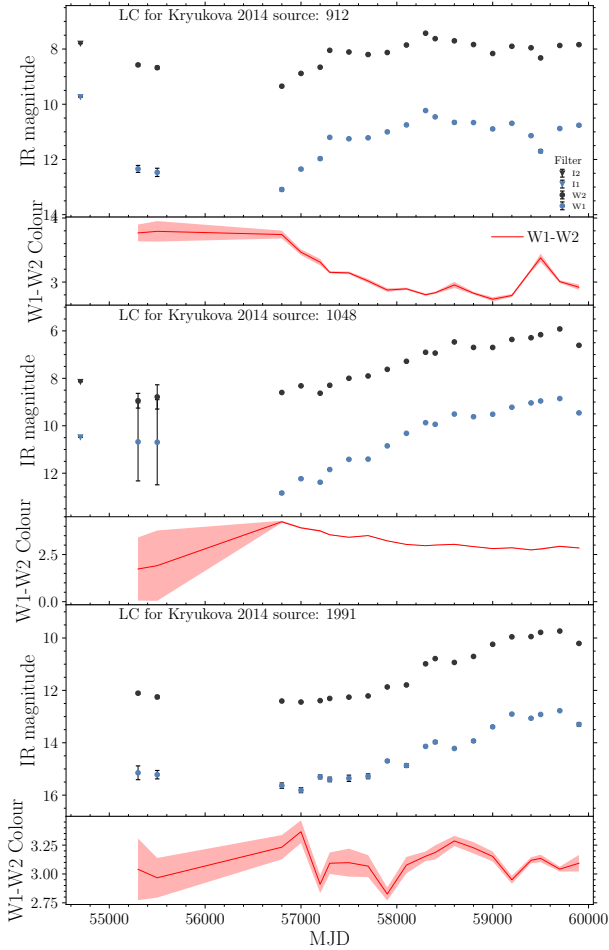
(Bradley et al. 2021) (lower limits being 16.9 mag, and 17.0 mag for sources 362 and 1964 respectively). The post-outburst light curves are displayed in Figure 2, both of which display the traditional fading behaviour of post-outburst FUors.

A second group within the LDEs are stars with extended rising times (greater than 3 years) before reaching their photometric maxima, these are Sources 912, 1048, and 1991 in Figure 3 (as well as Source 880 in Figure B1). It is worth noting that sources 880 and 912 do seem to have faded from earlier observations, so there is a chance that these two systems may be 'dippers'. These slow-rising infrared outbursts have been observed infrequently before (albeit prior to a higher amplitude outburst), such as the FUor Gaia17bpi (Hillenbrand et al. 2018), SSTgbs J21470601+4739394 (Ashraf et al. 2024), and VVVv721 (Contreras Peña et al. 2017b,c). This may suggest that the trigger for the outburst is driven by MRI (see Cleaver et al. (2023) for simulations of the low-power Gaia17bpi-like FUor outbursts). Outbursts with rising times on the order of a decade (as seen here) are predicted in the flyby-triggered models of Borchert et al. (2022a), whose authors related these to outbursts of lower accretion rate, but feeding from a reservoir of material at a larger rotation radius, on the order of 40-50 AU.
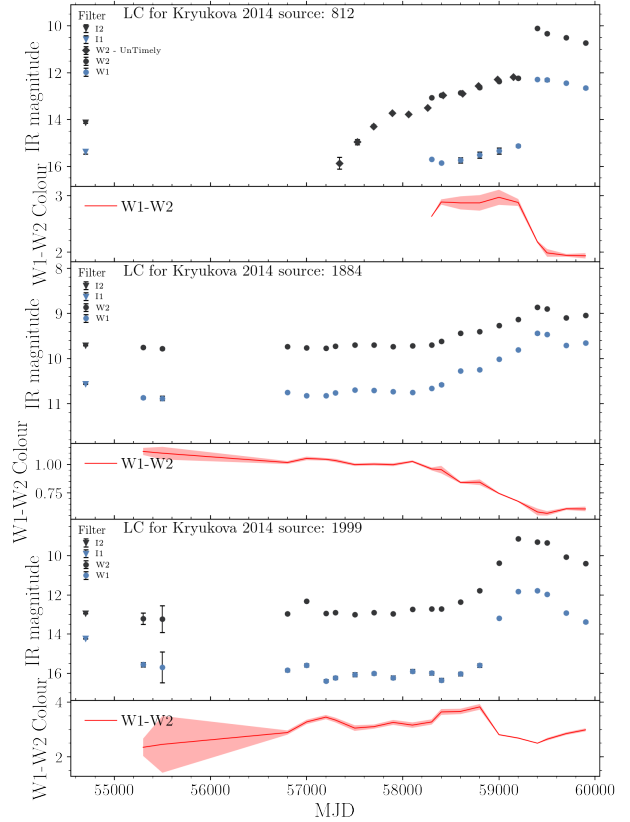
**Figure 3.** NEOWISE $W1$ & $W2$ light curves for three of the candidate eruptive variables with longer duration rise times. Each plot also contains a $W1 - W2$ colour indicator (red line), with the error included as the pink-shaded region.

### 3.1.3 YSOs with Short-Duration Outbursts

In total, there are 11 sources in this category, with the duration of outbursts less than two years. Among them, seven stars have multiple bursts (four of these are semi-regular, see Figure 5) and four others only have a single burst. The rest of the light curves are shown in Figures 6 & B2. There are no clear trends within this group, with a broad spread in amplitude, burst duration and colour behaviour.

Some sources of note in this selection are discussed below:

• Source 12 has four aperiodic outbursts with > 1 mag in $W2$-band amplitude. Unlike a typical EXor, Source 12 has redder-when-brighter colours, although given the large spectral index (1.03) this could be a result of reprocessing of more of the accretion luminosity into the MIR.

• Source 185 has four quasi-periodic outbursts that each last for ∼ 500 days (one of which is ongoing). We do not perceive the star to be a 'dipper' because of the irregularity of the bursts (which could not be reliably fitted by normal period-finding routines), which would normally - although not guaranteed to - be periodic if caused by extinction from orbiting material. There is a chance that this object might represent contamination from an evolved star (such as a long-period variable), although these stars MIR light curves are usually more regular than seen here.

**Figure 4.** NEOWISE $W1$ & $W2$ light curves for three of the candidate eruptive variables with shorter duration, FUor-like outbursts. Each plot also contains a $W1 - W2$ colour indicator (red line), with the error included as the pink-shaded region. Source 812 also contains W2 data from the UnTimely catalogue (Meisner et al. 2023).

• Source 232 has a recent outburst, in addition to the one previously identified in the UGPS survey (included within Lucas et al. 2017). We will discuss it in more detail in §3.1.4.

• Source 333 is of note from an additional long-duration outburst of 1.55 mag in $W1$, which has been ongoing since April 2019, although it reached its peak after ∼ 600 days. This burst was accompanied by a small reduction in the $W1 - W2$ colour, which was 2.13 at the start of the burst but fell to 1.50 at the maxima, and it continued to fall after the photometric maxima.

• Source 1626 (Fig 6, bottom panel) has the largest single outburst amongst the short-duration sources at 2.37 mag in $W1$, which combines with a slight blueing $W1 - W2$ colour of 0.28. The single large burst lasts only for ∼ 500 days, all of which are indicative of an EXor-type eruption.

### 3.1.4 Source 232

Source 232, also known as GPSV28 (Contreras Peña et al. 2014) and IRAS 20226+4206, was observed to have probable outburst in December 2008 with $\Delta K_s = 1.0$ mag, originally detected by the UGPS survey (included as Source 463 in Lucas et al. (2017)), the amplitude increases to $\Delta K_s = 1.56$ mag when including 2MASS photometry. Additionally, it has two spectroscopic follow-up observations using Gemini/NIFS (2015) and Subaru/IRCS (2017). These spectra are shown in Figure 7, which were acquired ∼4 and ∼6 years after the previous outburst. The spectra show notable differences in
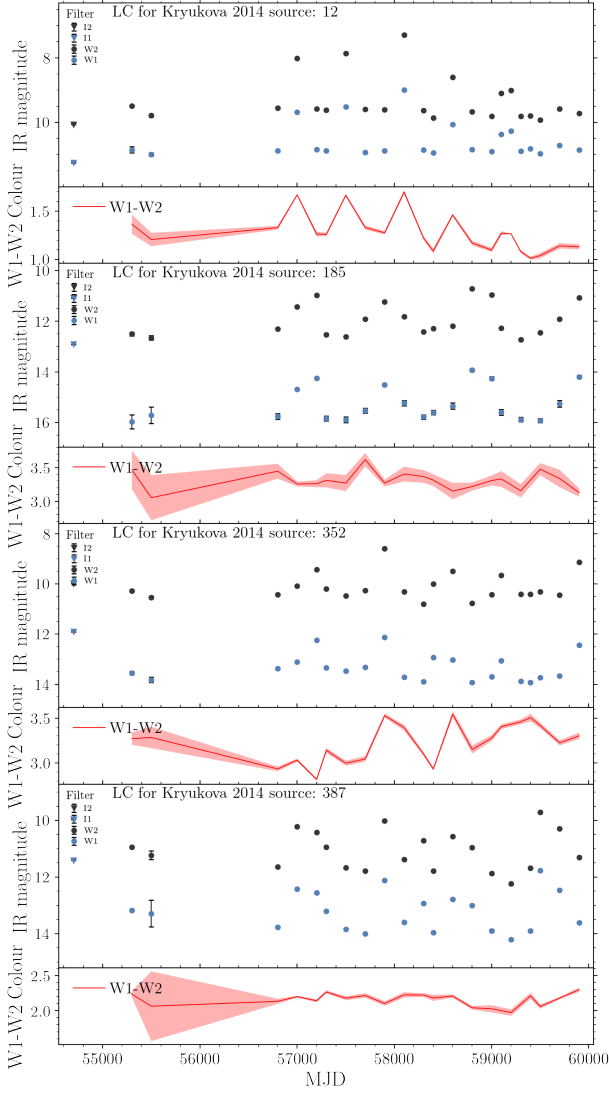
**Figure 5.** NEOWISE *W*1 & *W*2 light curves for the four semi-regular repeating short duration outbursts.



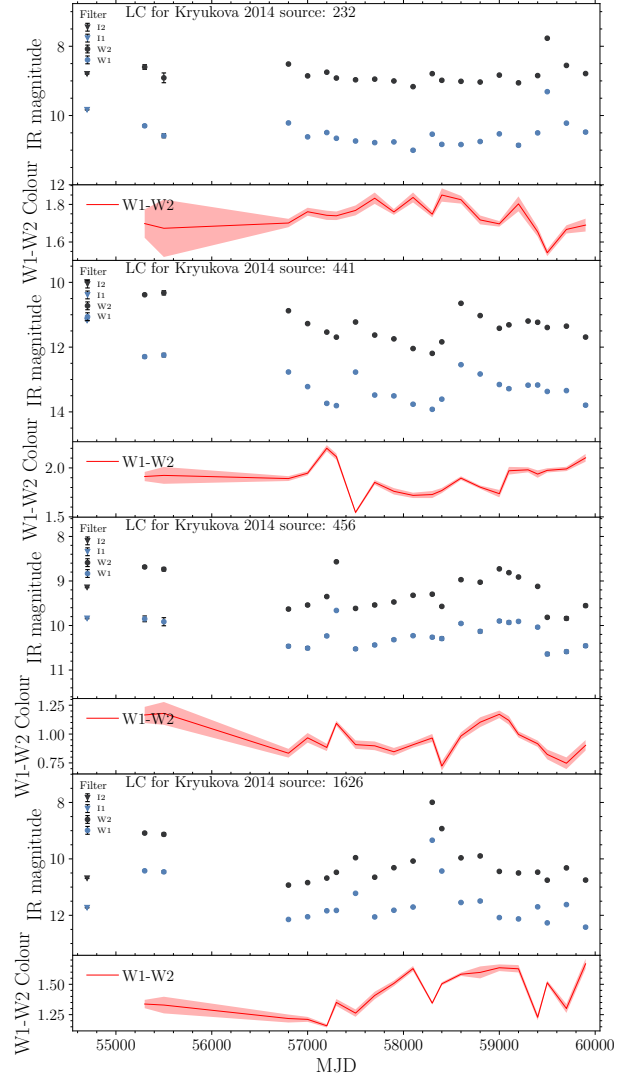**Figure 6.** NEOWISE *W*1 & *W*2 light curves for four of the short-duration outbursts that have only one or two eruptive events.

the emission line ratios, wherein the 2015 spectrum has more prominent $H_2$ lines (S(1) and S(0)) than H I, and a clear Na I doublet. The implication is that flux is a combination of the stellar photosphere, the inner accretion disk and outflows (traced by $H_2$). By the 2017 the spectrum is dominated by the Br$\gamma$ emission line, with a 3.98±0.61 Å (from −1.98 ± 0.58 Å, to −5.95 ± 0.2 Å) increase in equivalent width from the previous spectrum. Considering that this change implies an increase in the accretion rate, we speculate that a higher proportion of the observed flux is from the hot inner accretion disk, hence why emission lines associated with the accretion streams (Na I) are now significantly veiled by the continuum. Whilst the initial outburst of Source 232 was not fully captured by the WISE light curves, a second burst (Δ*W*1 = 1.4 mag) was observed between 2021 and 2022, making clear that this star has EXor-like behaviour.

### 3.1.5 *Eruptive YSOs with Ambiguous Outburst Durations*

The final three stars in this sample have ongoing outbursts, that are yet to reach the plateau, making it a challenge to determine a likely outburst duration (See Figure C3 for light curves). Source 2003 is

characterised by a large amplitude, 5.1 mag in W1, and colour change of over 1 mag to the blue in $W1 - W2$ during the burst, both of which are common among FUor-type stars. With the outburst being unfinished, there is a possibility of it being one of the largest MIR outbursts yet detected for a FUor.

The remaining two stars in the group, sources 1738 & 1769, display similar long-term trends. Each star's light curve contains a small, short-term increase in brightness, before a visibly longer-term outburst (ongoing). No other stars in the sample show such activity, and as yet the nature of the current outbursts is unknown.

### 3.2 Cygnus-X YSOs without [24] detections, from SPICY

Among the sample of the SPICY members, 402 stars have amplitudes of > 1 magnitude in either *W*1 or *W*2-band. We chose 1 mag as the threshold for inspection because MIR amplitudes are often a factor of 2 lower in amplitude than those seen in optical band-passes, and as such this corresponds to ≈2 mag, a little lower than the guidelines for an outburst as laid out by Fischer et al. (2022). The majority of the 402 stars showed single-epoch dipping events (likely extinc-

**Table 2.** 35 EV candidates found in SPICY with amplitude >1 mag

| SPICY ID | RA (deg) J2000 | Dec (deg) J2000 | $\Delta W1$ mag | $(W1 - W2)_{min}$ mag | Colour Behaviour | SED Class |
|---|---|---|---|---|---|---|
| 107699 | 304.0523 | +39.0873 | $1.025 \pm 0.010$ | 0.321 | RWB | Class II |
| 107742 | 304.1969 | +39.3892 | $1.054 \pm 0.010$ | 1.338 | BWB | Class II |
| 107855 | 304.3484 | +39.3052 | $0.969 \pm 0.008$ | 0.550 | No Change | Class II |
| 108504 | 305.3081 | +38.9968 | $1.125 \pm 0.013$ | 0.441 | RWB | Class II |
| 108553 | 305.3903 | +40.8526 | $0.855 \pm 0.017$ | 0.698 | RWB | Class II |
| 108835 | 305.7091 | +40.5112 | $1.338 \pm 0.046$ | 0.786 | BWB | Class II |
| 109025 | 305.9034 | +39.5591 | $0.875 \pm 0.006$ | 0.103 | RWB | Class III |
| 109259 | 306.1053 | +42.4036 | $1.233 \pm 0.014$ | 1.091 | BWB | Class II |
| 109392 | 306.1617 | +38.5000 | $1.904 \pm 0.015$ | 0.332 | RWB | Class II |
| 109705 | 306.4289 | +38.5806 | $4.121 \pm 0.021$ | 1.171 | BWB | FS |
| 109973 | 306.6403 | +39.6054 | $0.817 \pm 0.021$ | 0.345 | RWB | Class II |
| 110521 | 307.0781 | +39.4852 | $0.836 \pm 0.007$ | 0.157 | RWB | Class II |
| 110601 | 307.1598 | +38.8962 | $0.931 \pm 0.010$ | 0.416 | RWB | Class III |
| 110991 | 307.4678 | +40.4054 | $1.315 \pm 0.008$ | 0.713 | RWB | Class II |
| 111048 | 307.5187 | +40.3839 | $1.677 \pm 0.011$ | 0.025 | RWB | Class II |
| 111336 | 307.7453 | +40.5380 | $1.522 \pm 0.036$ | -0.124 | RWB | Class II |
| 111413 | 307.7927 | +40.4144 | $1.165 \pm 0.023$ | 0.443 | RWB | FS |
| 111739 | 307.9553 | +38.9405 | $1.810 \pm 0.067$ | 1.346 | BWB | ? |
| 111836 | 307.9984 | +41.0660 | $1.125 \pm 0.014$ | 0.821 | RWB | Class II |
| 111892 | 308.0221 | +42.8133 | $0.876 \pm 0.008$ | 1.050 | BWB | FS |
| 112458 | 308.2766 | +40.7189 | $0.616 \pm 0.057$ | -0.420 | RWB | Class II |
| 112533 | 308.3147 | +41.0470 | $1.561 \pm 0.018$ | 0.007 | RWB | Class II |
| 112884 | 308.4971 | +41.4482 | $0.614 \pm 0.011$ | 0.180 | RWB | Class II |
| 112979 | 308.5504 | +40.7098 | $1.201 \pm 0.006$ | 0.442 | RWB | Class II |
| 113094 | 308.6131 | +42.2315 | $1.672 \pm 0.001$ | 0.902 | BWB | Class II |
| 113145 | 308.6433 | +41.1734 | $1.489 \pm 0.015$ | 0.643 | RWB | Class II |
| 113564 | 308.9150 | +41.8482 | $1.550 \pm 0.016$ | 0.609 | Varied | Class II |
| 113803 | 309.0589 | +41.1173 | $0.904 \pm 0.009$ | 0.166 | RWB | Class III |
| 113865 | 309.0924 | +42.4434 | $1.043 \pm 0.049$ | -0.100 | Varied | FS |
| 113929 | 309.1289 | +39.6458 | $0.940 \pm 0.005$ | 0.441 | RWB | Class II |
| 114037 | 309.1980 | +42.6153 | $1.001 \pm 0.051$ | -0.018 | Varied | Class II |
| 114471 | 309.5422 | +42.2826 | $1.371 \pm 0.015$ | 0.417 | BWB | Class II |
| 114590 | 309.6542 | +42.5540 | $1.603 \pm 0.034$ | 0.542 | RWB | FS |
| 115546 | 310.4321 | +39.6725 | $0.662 \pm 0.023$ | 0.732 | RWB | FS |
| 115613 | 310.5619 | +39.7890 | $1.158 \pm 0.010$ | 0.777 | No Change | FS |

The colour behaviour column notes how the $W1 - W2$ colour changes during the eruptive portions of the light curve: BWB means the source is bluer-when-brighter (much like traditional EXors), RWB indicates redder-when-brighter behaviour, and "Varied" notes stars whose colour behaviour changes over the total duration of the light curve. YSOs with $W1$ amplitudes under 1 mag have $\Delta W2 > 1$ mag.
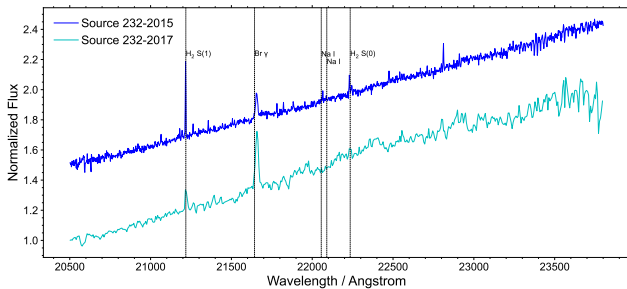


**Figure 7.** $K$ and $K'$ bandpass spectra for Source 232, taken in 2015 and 2017. Note the absence of lines from sodium in the 2017 spectrum, normally seen as a tracer of the accretion stream.

tion induced) or repeating redder-when-brighter 'dipper' behaviour. We then manually selected 35 EV candidates (see Table 3.1.5), including seven FS sources, 24 Class II YSOs, and three Class III YSOs. An additional source is considered uncertain (it lacks photometry in multiple *Spitzer* bandpasses), although its average WISE colour ($W1 - W2 = 1.66$) is comparable to the bluer Class I sources from section 3.1.1. Across the sample of EVs, 23/35 stars show the redder-when-brighter trend in their $W1 - W2$ colour during outburst. Applying the outburst duration-based classifications defined in §3, we find 30 SDEs, one IDE, two LDEs, and two sources of ambiguous classification.

### 3.2.1 New FUor-type/Long Duration Eruptive YSOs

The outburst detection code described in §2 located one star (SPICY 114590) with a shape comparable to that of an archetypal FUor (although the rise time is still on the longer scale, more similar to the VVV identified FUors), although it has a peak amplitude of < 2 mag (see Figure 8). The MIR colour behaviour of SPICY 114590 is different to that seen in the FUor candidates in §3.1, as this object gets redder during the outburst. The low amplitude is not unexpected in the general sense, as it can be predicted by outburst models for YSOs with already enhanced accretion rates (see Figure 1 in Hillenbrand & Rodriguez 2022, with the caveat that this was for a sun-like star).

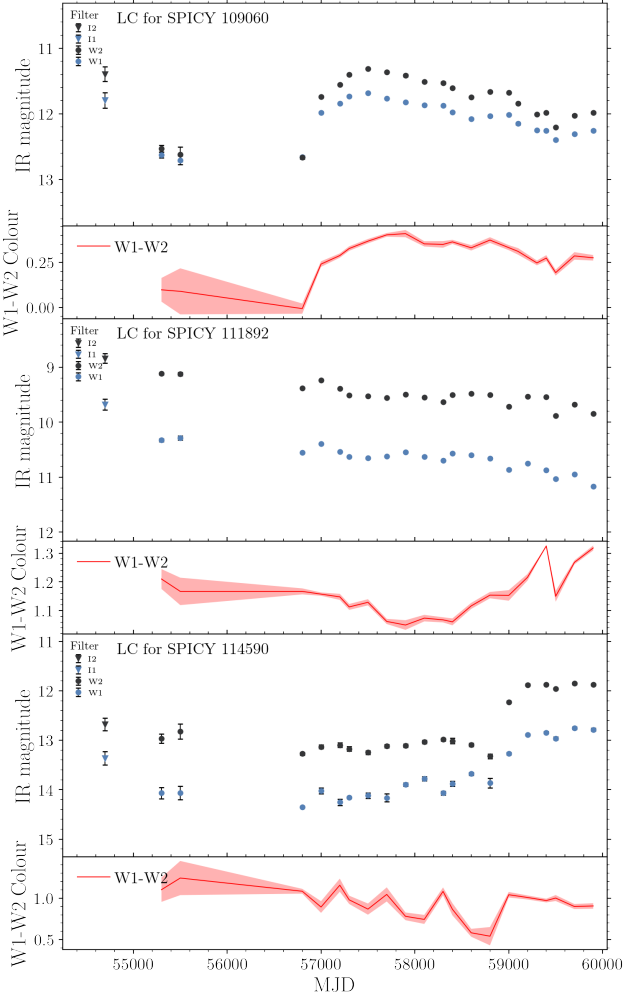SPICY 111892 has been previously identified as a candidate EV in

**Figure 8.** NEOWISE $W1$ & $W2$ light curves for three FUor candidates from the SPICY selected Class II/Flat-spectrum sources.
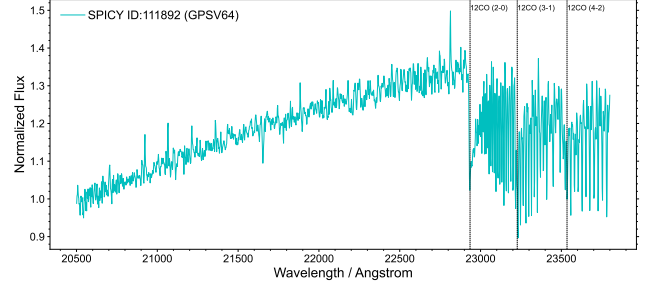


**Figure 9.** Gemini/NIFS spectrum for SPICY 111892. The spectrum is FUor-type, with a featureless red continuum and strong $^{12}$CO absorption features.

### 3.2.2 New EXor-like/Short Duration Eruptive YSOs

Of the 35 EV candidates in this group, 86% (30) have short-duration outburst events, many of which are similar to EXor-like YSOs. In line with the known diversity of these systems, we observed significant variation in the light curve morphologies, with differences in burst duration, amplitude, colour and repetition. We present four examples in Figure 10 that illustrates the variety (the rest can be seen in Appendix D).

SPICY 113094 displays quasi-periodic behaviour at a roughly 550 days period[3], with each burst of up to 1.6 mag and bluer colours during the photometric maxima. This is characteristic of stars such as SPICY 116663 (Kuhn et al. 2021) and periodic outbursting candidates discovered in VVV (Guo et al. 2022), albeit with a longer period than most examples.

SPICY 110521 shows repeating burst behaviour, although without any clear periodicity, effectively ruling out periodic occultation by dust. With outbursts of over 1 mag and colours that redden with increases in luminosity, it is however unlike the typical behaviour of EXors Lorenzetti et al. (see 2012), wherein colours are often expected to become bluer during outbursts. The behaviour seen in SPICY 110521 is commonly seen in this sample: 20 of 33 (60.6%) short duration (EXor-like) eruptive sources are redder in outburst.

SPICY 111336 also displays aperiodic, repetitive outbursts, but these are of differing amplitude, in contrast to many of the other repeating sources. The amplitudes in $\Delta W2$ range from $\sim 0.7$ mag to $\sim 1.5$ mag, although they are of a similar $\sim 400$ day duration (the duration is an upper limit owing to the wide sampling of NEOWISE). The range of amplitudes could also be a result of the sampling, with the peak of the outbursts being missed at several epochs, especially if the true period is less than 400 days.

The final EXor-like star to be discussed will be SPICY 112533, which is the most unusual star in this sample of later-stage YSOs. Seemingly there are two components to the light curve, with a potential long-term fading trend, which is separated into five detected outbursts each of between $\sim 0.8$ & 1.0 mag and $\sim 1.0$ & 2.0 mag in $W1$ & $W2$ respectively. Of additional note is the single outburst of at least 900 days (between 2016 and 2018) which bears little resemblance to other EXor-like bursts, owing to the comparatively short decay timescale as compared to the rise time.

Overall the sample of short-term variables is slightly biased towards sources with repetitive outburst behaviour, as is the case for 60.6% (20/33) of the sample. Whilst none of these are truly periodic, five of the stars display quasi-periodic bursts, with periods of over

UGPS by Contreras Peña (2015) and Lucas et al. (2017, as GPSV64). It displayed a 1.5 mag increase in $K_s$-band brightness between 2006 and 2009, which would be low for a FUor if this is the full amplitude of the event. However, the non-detection in earlier 2MASS images implies a longer rise time and a higher amplitude. The lower detection limit of the 2MASS $K_s$ image in which SPICY 111892 resides is calculated at 16.0 mag. This was calculated by running the `photutils` method called `ImageDepth`. This method takes the zero-point for the instrument, and a selection of magnitudes of stars in the image, and computes the lowest detectable flux for a given precision in sigma (quoted here are $3\sigma$ values) for a large number of randomly placed apertures. Thus the total $\Delta K_s$ has a lower limit of 4.0 mag, with a rising timescale of between $\sim$1000 and $\sim$4000 days. A follow-up spectrum was obtained in December 2014 (Figure 9) with Gemini/NIFS, which shows the mostly featureless red continuum and CO bandheads often associated with FUor spectra (the emission line at $2.282\mu m$ is likely spurious, as it had appeared in a large number of other YSOs in the same set of observations). See further examples of FUor-type spectra in Connelley & Reipurth (2018) and Guo et al. (2024a).

---

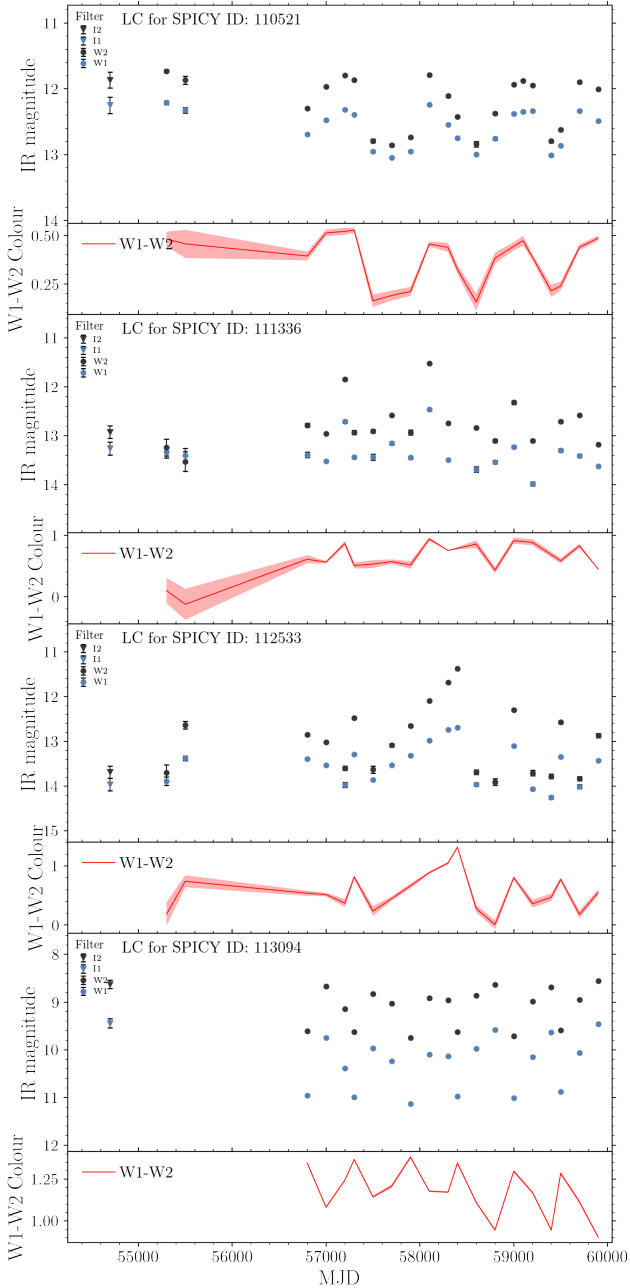[3] fitted using the `astropy LombScargle` function.

**Figure 10.** NEOWISE $W1$ & $W2$ light curves for four EXor candidate eruptive variables. These are selected because they demonstrate a wide range of behaviours and outburst durations. Of particular note is Source 112533, which had periodic small outbursts after a much larger, long-duration event.

400 days (the lowest that can be reliably identified with NEOWISE given the sampling).

## 4 DISCUSSIONS

### 4.1 Comparison of Embedded FUor Candidates with Classical FUors

Given the comparatively low number of known FUor-like stars, our discovery of 13 (these being the stars with FUor-type light curve morphologies or spectra) potential new candidates within a single
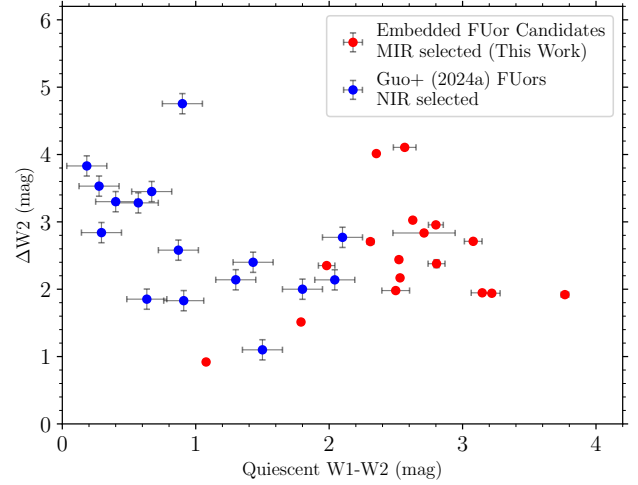
**Figure 11.** $W2$-band amplitude against quiescent $W1$-$W2$ colour for EVs discussed in §3.1. The NIR selected FUors are adopted from Guo et al. (2024a).

SFR warrants additional investigation. Given that our main sample was of the most embedded EVs within Cygnus-X, comparing their MIR behaviour to that of FUors discovered via a 'traditional' optical outburst could reveal differences between the two populations.

Guo et al. (2024a) provided a selection of FUors discovered by the near-infrared time series and further confirmed by follow-up spectroscopic observation. They found a negative correlation between the $\Delta W2$ and quiescent $W1 - W2$ colour (Fig 11 - blue points), whereas this does not agree with the long-duration EVs in our sample (Fig 11 - red points). The correlations were tested by performing Kendall $\tau$ tests on each sample, finding the NIR selected sources to have $\tau = -0.42$, compared to $\tau = 0$ for the MIR selected EVs from this work. Our EVs from Kryukova+ seem to have no correlation between $\Delta W2$ and $W1 - W2$, although all still show the common bluer-when-brighter colour behaviour during the outburst, similar to FUors. The figure also places the slowly rising eruptive variables amongst the FUor candidates, giving further weight to our hypothesis that these sources are YSOs that are building up to a FUor-type outburst (which may be optically detectable), in a similar vein to Gaia17bpi.

The reasoning for the break in the correlation of the colour/amplitude relation for the embedded sources is not yet fully clear, although a thicker envelope (and thus redder quiescent colours) might imply that we are seeing greater reprocessing of the accretion luminosity into the MIR, inflating the observed amplitude.

### 4.2 Comparing the Rates of Eruptive Behaviour Between Embedded and Non-Embedded Sources

By having a control sample of known YSOs, we can compare both the detection rates and amplitudes of eruptive variability for our embedded YSOs to those of the less embedded or more evolved sources within Cygnus-X. The comparisons between the frequency density and amplitude for our samples are shown in Figure 12, with embedded Class I sources in the left panel, and FS/Class II sources in the right. The embedded sources have a higher proportion of high-amplitude variables than the later stage sources, as 22.46% of Class I YSOs (From the $24\mu m$ selected sample) have $\Delta W1 > 1$ mag whilst just 4.94% FS/Class II YSOs (the SPICY sample) reach the same amplitude. We note that only a proportion of these variables
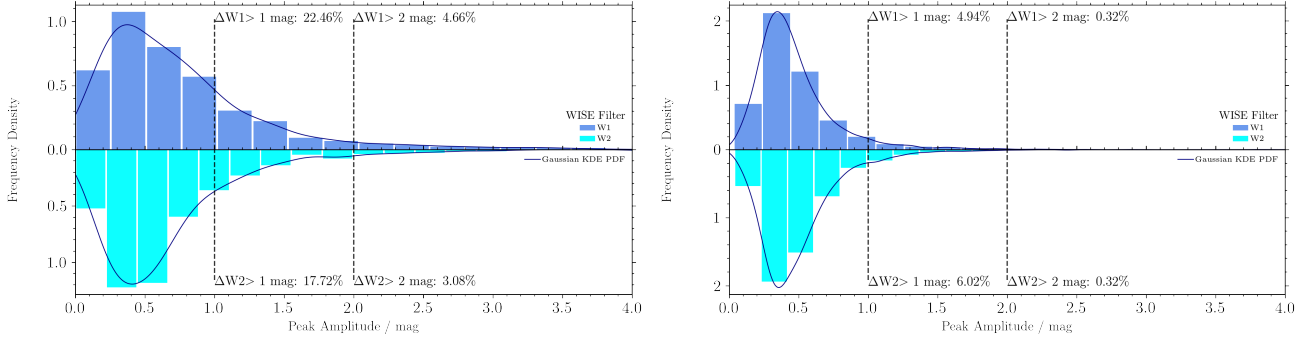
**Figure 12.** Histograms displaying peak amplitudes in $W1$ & $W2$ for both of the two samples discussed in Section 3. The left plot is the [24] detected sample, and the SPICY selected C2 and FS sources are in the right panel. Each individual histogram is presented with a probability distribution function, created by performing a Gaussian kernel density estimation.
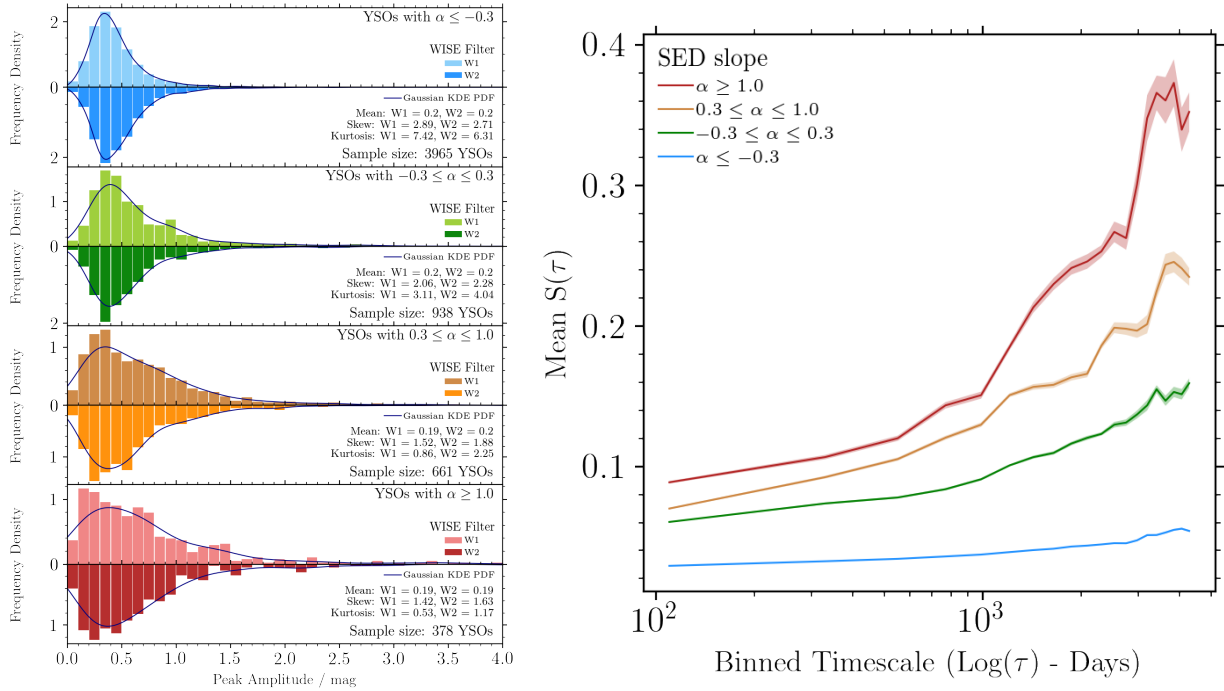


**Figure 13.** *Left:* $W1$ and $W2$ amplitude histograms for the combined YSO sample, split by SED slope class ($\alpha$). *Right:* Structure functions across a range of timescales for the combined YSO sample. Each point is the median structure in each timescale bin, averaged for both $W1$ and $W2$. These are once again separated by the value of the $\alpha$ parameter for the SED slope.

are eruptive, with large numbers of dippers, short-term variables and stars on long-term fading trends. Nevertheless, the fading sources may well be eruptive YSOs, wherein a large outburst has happened before our observation window and we are now witnessing the post-outburst cooling phase

To test the significance of these results, we performed a Mann-Whitney U (MW-U) test, between both samples. Because the sample of FS/Class II sources is substantially larger than that of Class I sources, we performed the MW-U test on two equal-sized samples drawn from distributions defined by a Gaussian kernel density estimation (fitted to all four histograms in Figure 12). Both of these routines are carried out in `Python`, using the `gaussian_kde` routine in `scipy.stats`. This test produced an average p-value of 3.46% over 10000 iterations and thus provided moderately statistically signifi-

cant evidence that these two samples were drawn from two different distributions.

From the perspective of YSO evolution, the above result is within expectation, as younger systems have a larger reservoir of material to accrete from. Massive discs with envelopes are also more likely to become unstable under gravity, especially when considering that flyby events are likely to be more common in younger (less bound) clusters. For further discussion of this idea, see Audard et al. (2014).

Given the potentially higher chance for outbursts, searching for EVs amongst younger systems specifically should result in a larger sample, especially of the rarer FU Ori-type objects. This falls into the long-held view that longer duration outbursts happen in younger systems (Hartmann & Kenyon 1996), given the long average length of FUor events. The differing morphologies among our long-duration outbursts also fit into the ideas of Quanz et al. (2007), which de-

scribe a possible evolutionary sequence for FUors, based upon their MIR features. The above point makes a strong case for follow-up spectroscopy at both near and mid-infrared wavelengths.

To further investigate the relationship between outburst amplitude and age for YSOs, we compared the combined sample of YSOs on the basis of the 0.8 - 12 $\mu$m spectral index ($\alpha$). Figure 13 shows the proportion of high amplitude variables increasing with $\alpha$, noting the decrease in kurtosis for the later stage YSOs indicates that the distribution becomes more centrally dominant (and thus lower amplitude on average).

We can also examine the timescales of the observed variability, i.e., the durations of individual variable events. For our sample we wish to identify any relationship between outburst duration and evolutionary stage, and thus we separate our sample of stars with > 1 mag variability by the same spectral index groups as before. We use structure functions as an analogue to timescale, as laid out in Sergison et al. (2020) and Lakeland & Naylor (2022), although similar tests for YSO variability were carried out in Findeisen et al. (2015).

$$S(\tau) = \langle [m(t) - m(t + \tau)]^2 \rangle \tag{5}$$

Where $S$ is the structure, $\tau$ is the timescale between two points in a light curve, $m$ is the apparent magnitude, and $t$ is the modified Julian date of any given point in the light curve. This function produces a measure of correlation between each point in a light curve for a range of time baselines (we use 12 bins ranging from ~100 days to ~10 years). In the right panel of Figure 13, we show that the signal is well correlated ($S$ is low) at the shortest timescales (here that is on the order of 3 months), and becomes less so as the timescale increases ($S$ is large). The implications here are that at shorter timescales it is easier to predict the next measurement in the time series (i.e. is less variable), and gets progressively more challenging at longer time baselines. It is worth noting that we do not see the higher $S$ values at the short timescales that Lakeland & Naylor (2022) attributed to measurement error and short-term variability because our data from NEOWISE have been averaged at the shortest time baselines. We do see the same 'Knee' feature at large $\tau$ for 3 of the groups however, which those authors attributed to a combination of long-term linear trends or a maximum variability timescale for YSOs.

From both of the above tests it seems apparent that long-duration, high-amplitude variability is more common for more heavily embedded (likely younger) YSOs, as has been suggested previously (see Contreras Peña et al. 2024).

## 5 SUMMARY

In this work, we have presented 68 candidate eruptive variable YSOs associated with the Cygnus X star-forming region, based on their decade-long mid-infrared NEOWISE light curves.

Amongst these are 9 YSOs with light-curve morphologies similar to those of FUors or V1647 Ori objects. This is in addition to 3 stars with previous NIR outursts and decaying MIR light curves, and an additional 4 YSOs with slower brightening phases, of a more type more reminiscent of V1515 Cyg. One final star has a currently ongoing >5 mag outburst for a total of 17 potential candidate FUors.

We also locate a large number of YSOs with short duration outbursts (some with EXor-like features) within both samples carried out, with 13 embedded Class I YSOs and 32 flat-spectrum or Class II stars. Compared with more evolved systems, we detected significantly more high amplitude (and eruptive) variables among the Class I YSOs (22.46%). This is especially true for the FUor type EVs, of which we have identified up to 16 candidate members, and several

have a less common, slow-rising character. Given the similarities between these objects and the pre-outburst light curves of several novel FUors, these 'slow-risers' might be further examples of FUors that outburst at earlier times in redder wavelengths.

Given this new population of eruptive young stars, follow-up observations are planned for those stars still at a state of high accretion rate and are thus bright in the near-infrared. This attempt may unveil any differences in accretion behaviour and disk/wind structure between the heavily embedded EVs and the traditional optical/NIR selected sources.

## DATA AVAILABILITY

The *WISE* and *Spitzer* data underlying this article are publicly available at the IRSA server https://irsa.ipac.caltech.edu/Missions/wise.html. Reduced spectra are provided at http://star.herts.ac.uk/~pwl/xxxx.

## REFERENCES

Acosta-Pulido J. A., et al., 2007, AJ, 133, 2020
Ashraf M., Jose J., Lee H.-G., Contreras Peña C., Herczeg G. J., Liu H., Johnstone D., Lee J.-E., 2024, MNRAS, 527, 11651
Audard M., et al., 2014, in Beuther H., Klessen R. S., Dullemond C. P., Henning T., eds, Protostars and Planets VI. pp 387–410 (arXiv:1401.3368), doi:10.2458/azu_uapress_9780816531240-ch017
Barentsen G., et al., 2014, MNRAS, 444, 3230
Beerer I. M., et al., 2010, ApJ, 720, 679
Bell K. R., Lin D. N. C., 1994, ApJ, 427, 987
Benjamin R. A., et al., 2003, PASP, 115, 953
Borchert E. M. A., Price D. J., Pinte C., Cuello N., 2022a, MNRAS, 510, L37
Borchert E. M. A., Price D. J., Pinte C., Cuello N., 2022b, MNRAS, 517, 4436
Bourdarot G., et al., 2023, A&A, 676, A124
Bouvier J., et al., 2007, A&A, 463, 1017
Bradley L., et al., 2021, astropy/photutils: 1.2.0, doi:10.5281/zenodo.5525286, https://doi.org/10.5281/zenodo.5525286
Briceño C., et al., 2004, ApJ, 606, L123
Clarke C., Lodato G., Melnikov S. Y., Ibrahimov M. A., 2005, MNRAS, 361, 942
Cleaver J., Hartmann L., Bae J., 2023, MNRAS, 523, 5522
Connelley M. S., Reipurth B., 2018, The Astrophysical Journal, 861, 145
Contreras Peña C. E., 2015, PhD thesis, University of Hertfordshire, UK

Contreras Peña C., et al., 2014, MNRAS, 439, 1829
Contreras Peña C., et al., 2017a, MNRAS, 465, 3011
Contreras Peña C., et al., 2017b, MNRAS, 465, 3011
Contreras Peña C., et al., 2017c, MNRAS, 465, 3039
Contreras Peña C., et al., 2023, Journal of Korean Astronomical Society, 56, 253
Contreras Peña C., Lucas P. W., Guo Z., Smith L., 2024, MNRAS, 528, 1823
Contreras Peña C., Johnstone D., Baek G., Herczeg G. J., Mairs S., Scholz A., Lee J.-E., Team T. J. T., 2020, Monthly Notices of the Royal Astronomical Society, 495, 3614
Cuello N., et al., 2019, MNRAS, 483, 4114
Drew J. E., et al., 2005, Monthly Notices of the Royal Astronomical Society, 362, 753
Findeisen K., Cody A. M., Hillenbrand L., 2015, ApJ, 798, 89
Fischer W. J., Hillenbrand L. A., Herczeg G. J., Johnstone D., Kóspál Á., Dunham M. M., 2022, arXiv e-prints, p. arXiv:2203.11257
Gaia Collaboration et al., 2023, A&A, 674, A1
Greene T. P., Lada C. J., 1996, AJ, 112, 2184
Guo Z., et al., 2021, MNRAS, 504, 830
Guo Z., et al., 2022, MNRAS, 513, 1015
Guo Z., et al., 2024a, MNRAS, 528, 1769
Guo Z., et al., 2024b, MNRAS, 529, L115
Hartmann L., Kenyon S. J., 1996, ARA&A, 34, 207
Hartmann L., Zhu Z., Calvet N., 2011, arXiv e-prints, p. arXiv:1106.3343
Hillenbrand L. A., Rodriguez A. C., 2022, Research Notes of the American Astronomical Society, 6, 6
Hillenbrand L. A., et al., 2018, ApJ, 869, 146
Hora J., et al., 2007, A Spitzer Legacy Survey of the Cygnus-X Complex, Spitzer Proposal ID #40184
Kiwy F., 2022, unTimely_Catalog_explorer: A search and visualization tool for the unTimely Catalog, Astrophysics Source Code Library, record ascl:2211.005 (ascl:2211.005)
Kobayashi N., et al., 2000, in Iye M., Moorwood A. F., eds, Society of Photo-Optical Instrumentation Engineers (SPIE) Conference Series Vol. 4008, Optical and IR Telescope Instrumentation and Detectors. pp 1056–1066, doi:10.1117/12.395423
Koenig X. P., Leisawitz D. T., 2014, The Astrophysical Journal, 791, 131
Kratter K., Lodato G., 2016, ARA&A, 54, 271
Kryukova E., et al., 2014a, AJ, 148, 11
Kryukova E., et al., 2014b, The Astronomical Journal, 148, 11
Kuhn M. A., de Souza R. S., Krone-Martins A., Castro-Ginard A., Ishida E. E. O., Povich M. S., Hillenbrand L. A., COIN Collaboration 2021, ApJS, 254, 33
Kuhn M. A., Benjamin R. A., Ishida E. E. O., de Souza R. S., Peloton J., Veneri M. D., 2023, Research Notes of the American Astronomical Society, 7, 57
Lakeland B. S., Naylor T., 2022, MNRAS, 514, 2736
Liu H., et al., 2022, ApJ, 936, 152
Lorenzetti D., et al., 2012, The Astrophysical Journal, 749, 188
Lucas P. W., et al., 2008, MNRAS, 391, 136
Lucas P. W., et al., 2017, Monthly Notices of the Royal Astronomical Society, 472, 2990
Lucas P. W., et al., 2024, MNRAS, 528, 1789
Mainzer A., et al., 2014, ApJ, 792, 30
McGregor P. J., et al., 2003, in Iye M., Moorwood A. F. M., eds, Society of Photo-Optical Instrumentation Engineers (SPIE) Conference Series Vol. 4841, Instrument Design and Performance for Optical/Infrared Ground-based Telescopes. pp 1581–1591, doi:10.1117/12.459448
Meisner A. M., Lang D., Schlegel D. J., 2018, AJ, 156, 69
Meisner A. M., Caselden D., Schlafly E. F., Kiwy F., 2023, AJ, 165, 36
Minniti D., et al., 2010, New Astronomy, 15, 433
Nayakshin S., Elbakyan V., 2024, MNRAS, 528, 2182
Nayakshin S., Cruz Sáenz de Miera F., Kóspál Á., Ćalović A., Eislöffel J., Lin D. N. C., 2024, MNRAS, 530, 1749
Quanz S. P., Henning T., Bouwman J., van Boekel R., Juhász A., Linz H., Pontoppidan K. M., Lahuis F., 2007, ApJ, 668, 359
Rygl K., et al., 2012, Astronomy & Astrophysics, 539, A79
Schlafly E. F., et al., 2018, ApJS, 234, 39
Scholz A., Froebrich D., Wood K., 2013, MNRAS, 430, 2910
Sergison D. J., Naylor T., Littlefair S. P., Bell C. P. M., Williams C. D. H., 2020, MNRAS, 491, 5035
Skrutskie M. F., et al., 2006, AJ, 131, 1163
Stauffer J., et al., 2014, AJ, 147, 83
Tokunaga A. T., et al., 1998, in Fowler A. M., ed., Society of Photo-Optical Instrumentation Engineers (SPIE) Conference Series Vol. 3354, Infrared Astronomical Instrumentation. pp 512–524, doi:10.1117/12.317277
Venuti L., et al., 2019, Technical report, X-shooter spectroscopy of young stars with disks The TW Hydrae association as a probe of the final stages of disk accretion ‹, https://arxiv.org/pdf/1909.06699.pdf. (arXiv:1909.06699v1), https://arxiv.org/pdf/1909.06699.pdf
Vorobyov E. I., Basu S., 2010, ApJ, 719, 1896
Whitney B., et al., 2011, in American Astronomical Society Meeting Abstracts #217. p. 241.16
Wright E. L., et al., 2010, AJ, 140, 1868
Zhu Z., Hartmann L., Gammie C., McKinney J. C., 2009, ApJ, 701, 620

## APPENDIX A:  OUTBURST TIMESCALE FITS WITH EMCEE

The plots below demonstrate the some of the results of fitting a characteristic FUor-type shape to a NEOWISE light curve. As mentioned in the text (§2.1) we use emcee to fit 3 light curve components (representing the start of the outburst, the main rising slope, and the post-outburst linear decay) with 5 free parameters. Candidates were marked for further investigation if the reduced mean square error (RMSE) was less than 0.15. This value has been selected initially because it allows the code to recover all the stars in the sample that visual inspection identified as FUor candidates, with reasonably typical light-curves. The code does not recover the stars with consistent (and fairly slow) rising slopes, such as Source 1048. In a sample of stars of this size, our fitting technique is of questionable utility, however it will be of use when examining larger populations for which visual inspection would be inefficient.

## APPENDIX B:  ADDITIONAL LIGHT CURVES FROM THE EMBEDDED YSO SAMPLE

Listed in this section are the light curves from the stars not mentioned directly in the text.

## APPENDIX C:  LIGHT CURVES FOR HIGH-AMPLITUDE CLASS I VARIABLE YSOS

## APPENDIX D:  LIGHT CURVES FOR HIGH AMPLITUDE VARIABLE YSOS FROM SPICY

Listed here are the NEOWISE MIR light curves for the EXor candidates discussed in section 3.2.

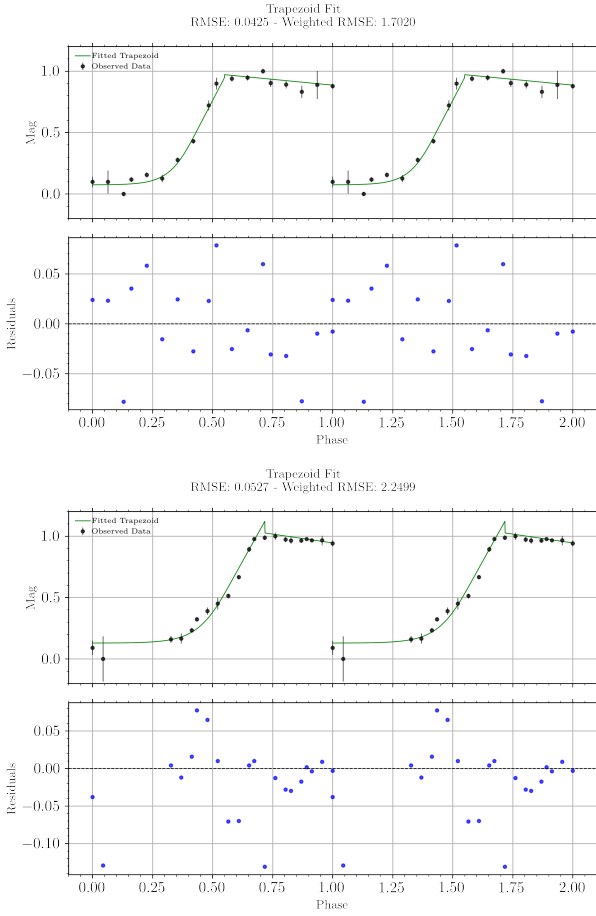This paper has been typeset from a TeX/LaTeX file prepared by the author.

**Figure A1.** NEOWISE light curves (black points) and the best fit FUor outburst model (green line) for the first two FUor candidates mentioned in the text, Sources 257 (top) and 294 (bottom). The plots display the light curves twice, from zero to two phase, owing to the code's utility in additionally fitting to periodic signals.
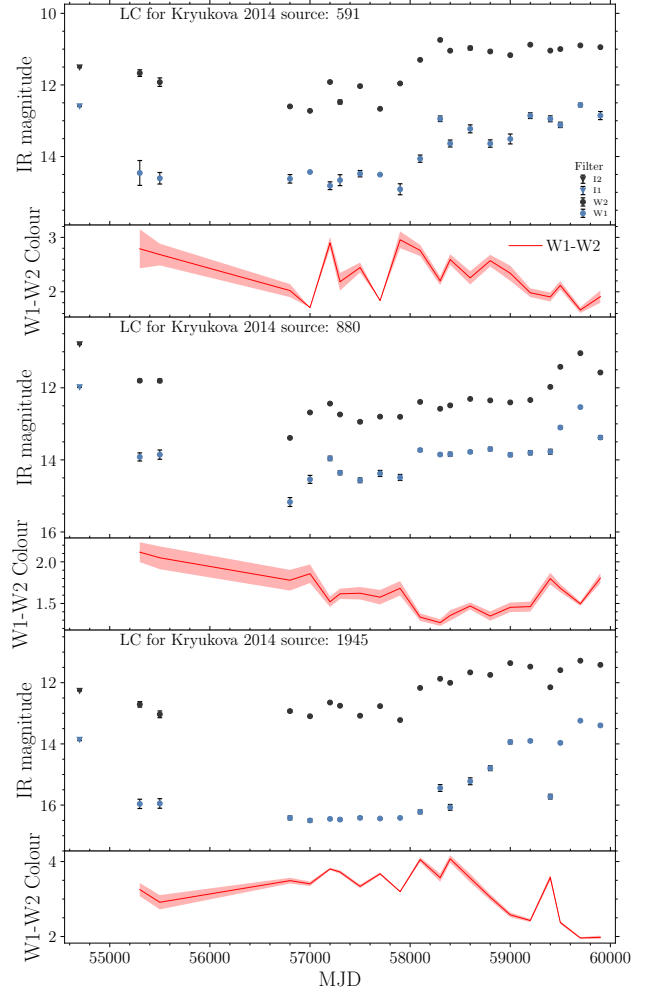


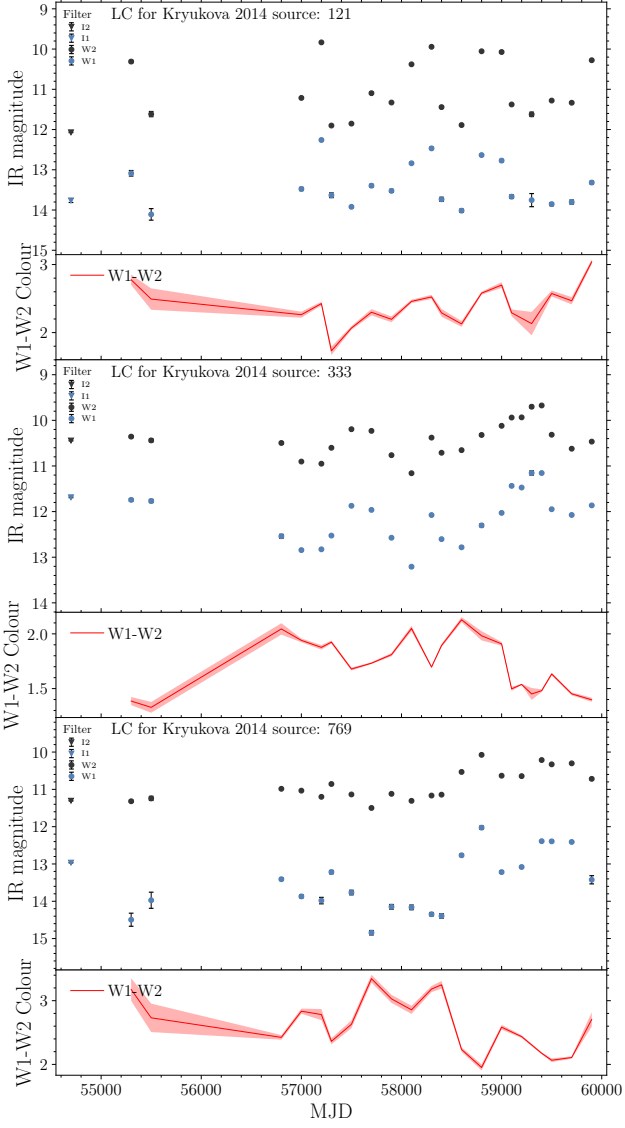**Figure B1.** NEOWISE $W1$ & $W2$ light curves for the 3 long duration sources not detailed within the main text.

**Figure B2.** NEOWISE *W*1 & *W*2 light curves for the short-term variables not discussed in the main text.
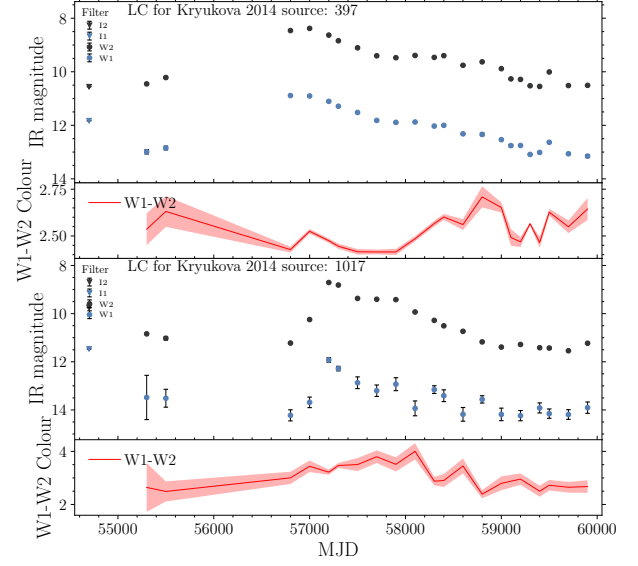
**Figure C1.** NEOWISE *W*1 & *W*2 light curves for two of the candidate eruptive variables with completed outbursts.
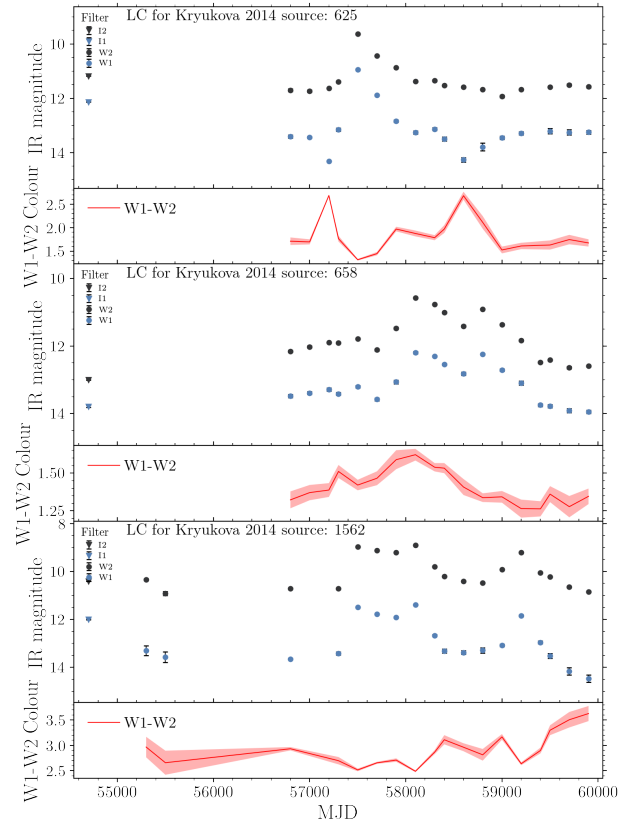
**Figure C2.** NEOWISE *W*1 & *W*2 light curves for three of the candidate eruptive variables with complex light curves.
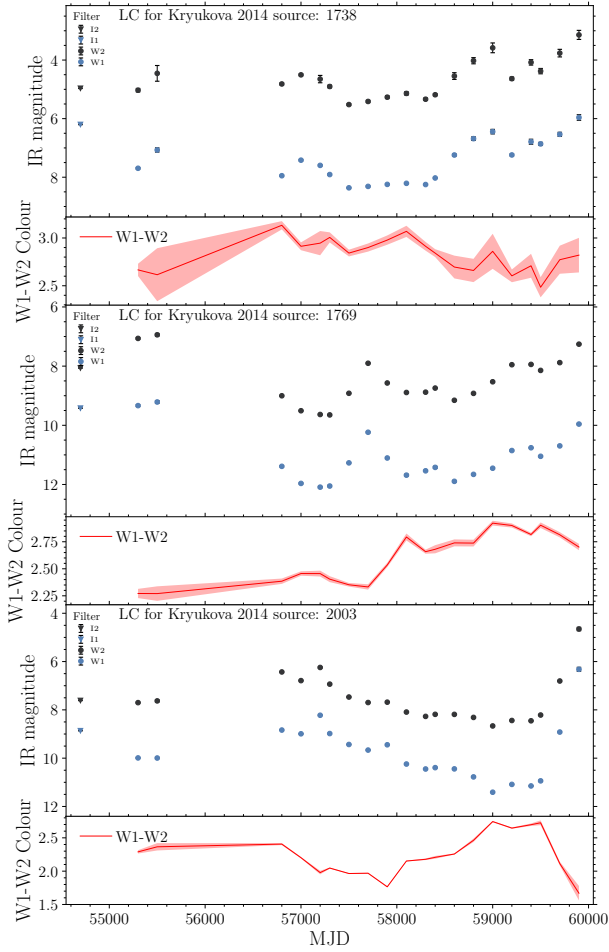
**Figure C3.** NEOWISE $W1$ & $W2$ light curves for the three stars with uncertain outburst durations.
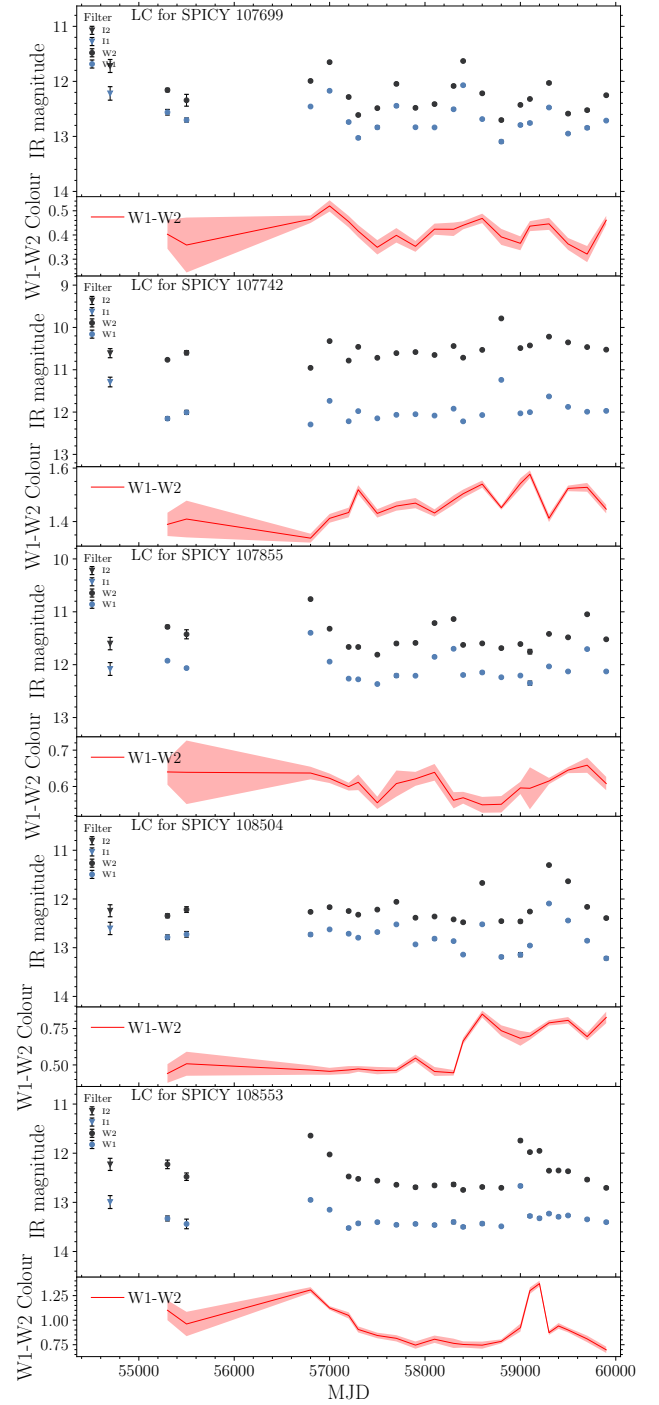


**Figure D1.** NEOWISE $W1$ & $W2$ light curves for the EXor candidates in the SPICY selected sample.
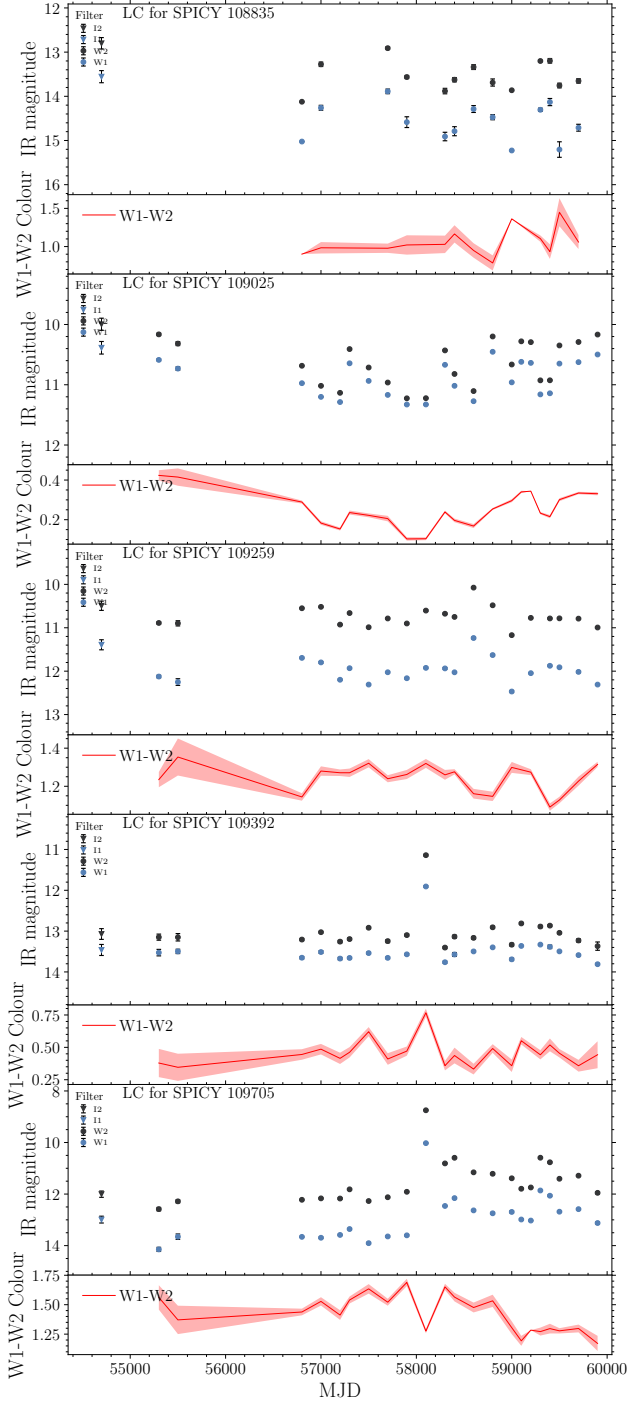
**Figure D2.** NEOWISE *W*1 & *W*2 light curves for the EXor candidates in the SPICY selected sample.
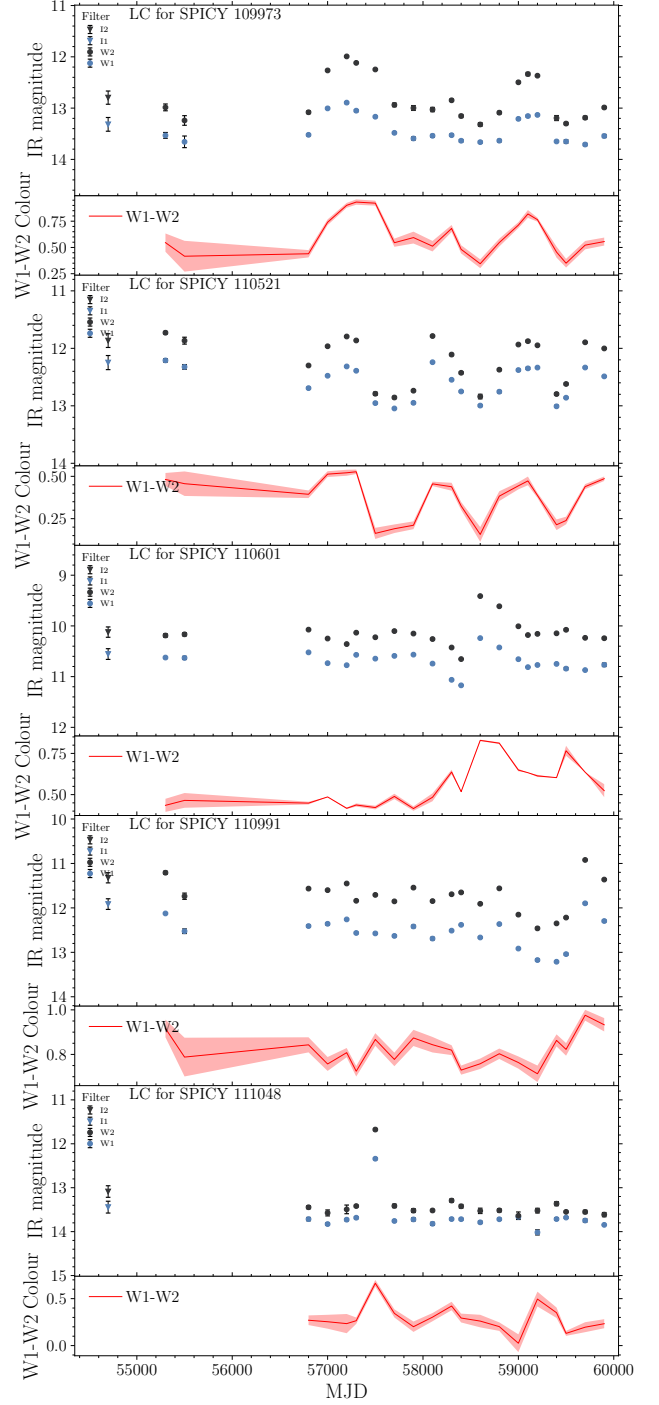
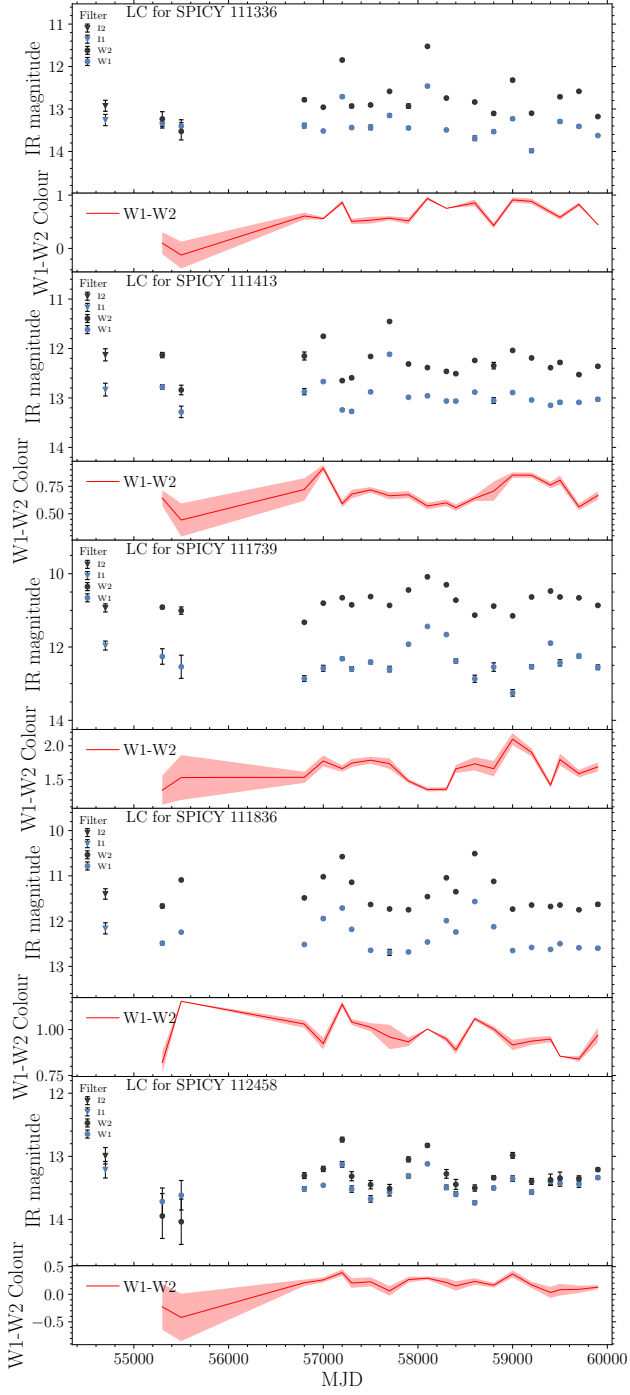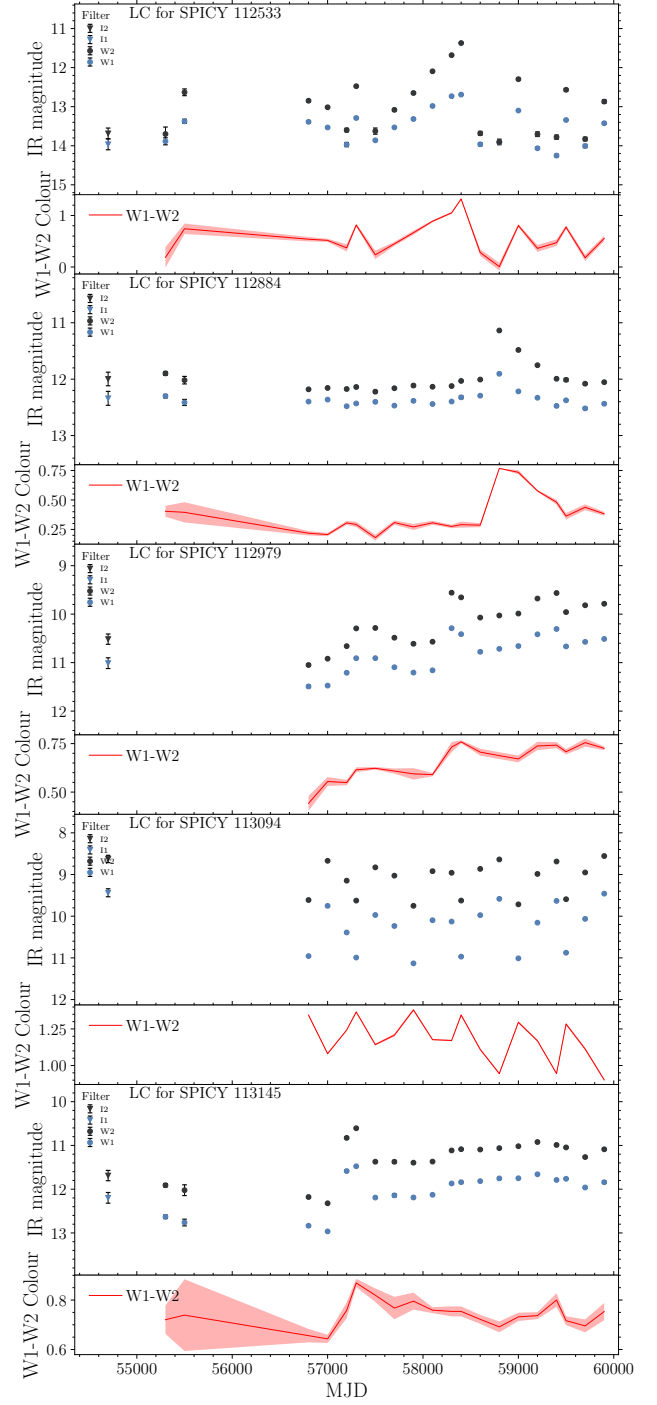**Figure D3.** NEOWISE *W*1 & *W*2 light curves for the EXor candidates in the SPICY selected sample.

**Figure D4.** NEOWISE $W1$ & $W2$ light curves for the EXor candidates in the SPICY selected sample.

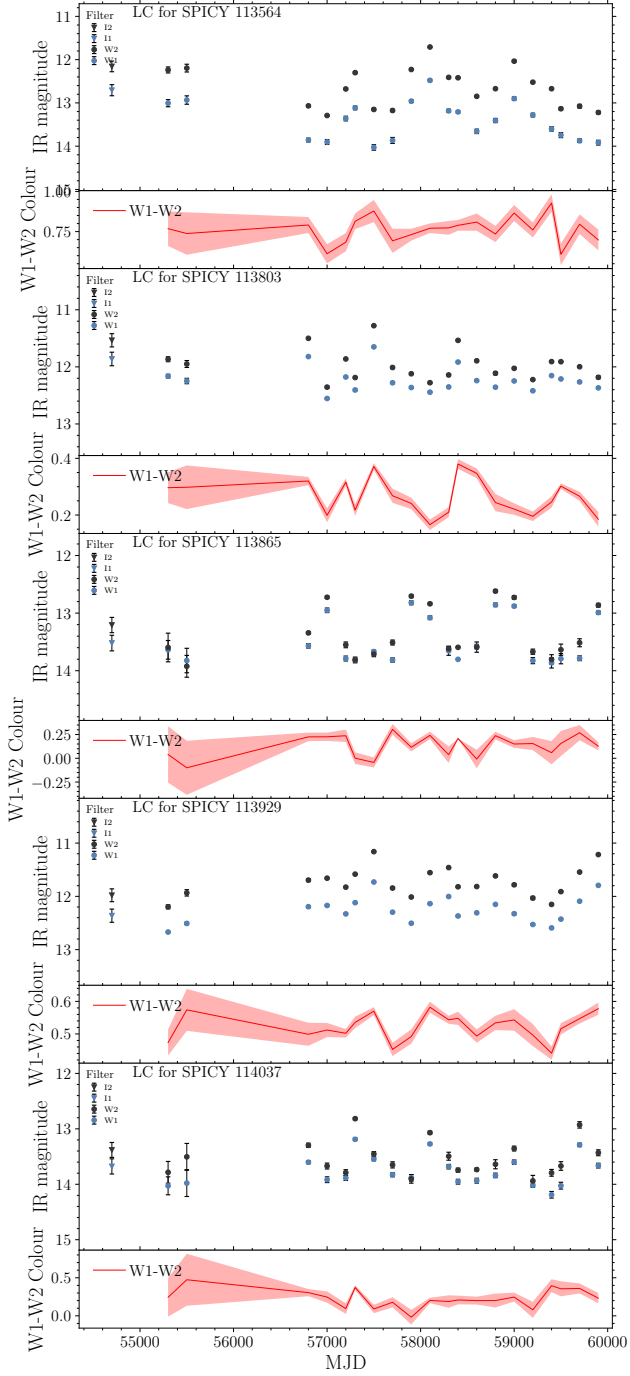**Figure D5.** NEOWISE $W1$ & $W2$ light curves for the EXor candidates in the SPICY selected sample.

**Figure D7.** NEOWISE *W*1 & *W*2 light curves for the EXor candidates in the SPICY selected sample.



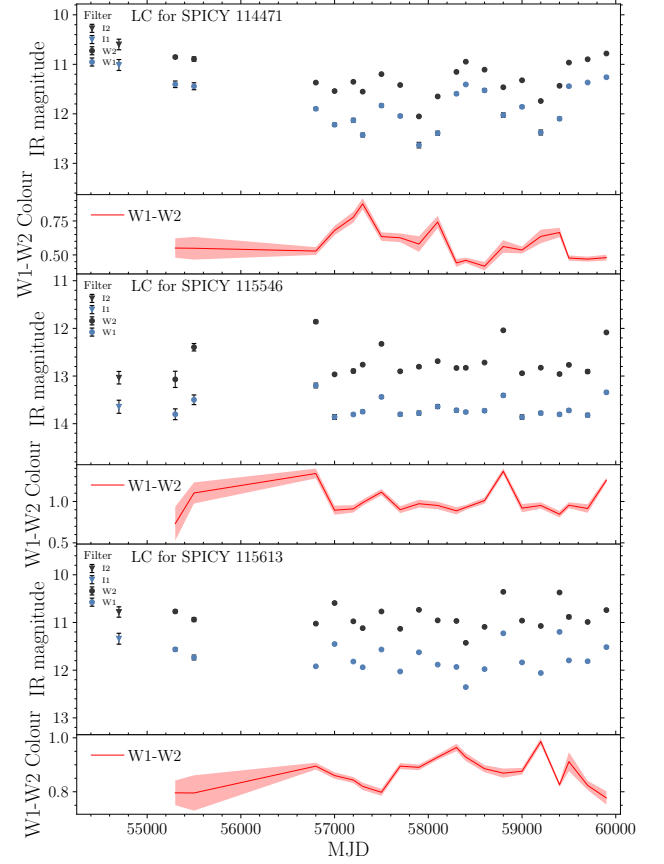**Figure D6.** NEOWISE *W*1 & *W*2 light curves for the EXor candidates in the SPICY selected sample.